Journal of
Medicinal Chemistry

Article

Discovery of MFH290: A Potent and Highly Selective Covalent Inhibitor for Cyclin-Dependent Kinase 12/13

Yao Liu, Mingfeng Hao, Alan Leggett, Yang Gao, Scott B Ficarro, Jianwei Che, Zhixiang He, Calla Olson, Jarrod A. Marto, nicholas Kwiatkowski, Tinghu Zhang, and Nathanael S Gray

J. Med. Chem., **Just Accepted Manuscript** • DOI: 10.1021/acs.jmedchem.9b01929 • Publication Date (Web): 05 Jun 2020

Just Accepted

is published by the American Chemical Society. 1155 Sixteenth Street N.W., Washington, DC 20036

Discovery of MFH290: A Potent and Highly Selective Covalent Inhibitor for Cyclin-Dependent Kinase 12/13

Yao Liu[⊥,†,‡], Mingfeng Hao[⊥,†,‡], Alan L. Leggett[⊥,†], Yang Gao[⊥,†], Scott B. Ficarro[⊥,†,§], Jianwei Che[⊥,†], Zhixiang He[⊥,†], Calla M. Olson[⊥,†], Jarrod A. Marto[⊥,†,§], Nicholas P. Kwiatkowski[⊥,†,], Tinghu Zhang[⊥,†,*], Nathanael S. Gray[⊥,†,*]*

[⊥]Department of Biological Chemistry and Molecular Pharmacology, Harvard Medical School, Boston, MA 02115, USA; [†]Department of Cancer Biology, Dana Farber Cancer Institute, 450 Brookline Avenue, Boston, MA 02215, USA; [§]Blais Proteomics Center, Dana Farber Cancer Institute, Harvard Medical School, Boston, MA 02215, USA;

KEYWORDS: CDK12/13 inhibitor, covalent inhibitor, cysteine 1039.

ABSTRACT: Genetic depletion of cyclin-dependent kinase 12 (CDK12) or selective inhibition of an analog-sensitive CDK12 reduces DNA damage repair gene expression, but selective inhibition of endogenous CDK12 is difficult. Here, we report the development of MFH290, a novel cysteine (Cys)-directed covalent inhibitor of CDK12/13. MFH290 forms a covalent bond with Cys-1039 of CDK12, exhibits excellent kinome selectivity, inhibits the phosphorylation of serine-2 in the C-terminal domain (CTD) of RNA-polymerase II (Pol II) and reduces the expression of key DNA damage repair genes. Importantly, these effects were demonstrated to be CDK12-dependent as mutation of Cys-1039 rendered the kinase refractory to MFH290 and restored Pol II CTD phosphorylation and DNA damage repair gene expression. Consistent with its effect on

DNA damage repair gene expression, MFH290 augments the anti-proliferative effect of the PARP inhibitor, Olaparib.

INTRODUCTION

Cyclin Dependent Kinases, or CDKs, are an intensively investigated family of evolutionarily conserved protein kinases that orchestrate the cell cycle and gene transcription[1, 2]. Human cells encode 20 distinct CDKs which possess highly similar ATP-binding pockets thereby making the development of selective CDK inhibitors challenging[3]. Despite these difficulties, some CDKs can be targeted quite selectively, such as CDK4/6 by the FDA approved drug palbociclib, based on recognition of unique combinations of residues in the ATP-pocket. A more recently explored strategy has been to exploit uniquely positioned cysteine residues with reactive, electrophile-modified inhibitors as exemplified by the development of the CDK7/12/13 inhibitor THZ1 (**Figure 1**) which targets an unusual cysteine 312 located on a loop that traverses the inhibitor binding pocket[4]. Further structure-guided optimization of THZ1 resulted in the development of the selective CDK12/13 inhibitor THZ531[5] (**Figure 1**), which targets a spatially distinct cysteine residue (Cys1039 for CDK12 and Cys1017 for CDK13).

CDK12 and the highly homologous protein CDK13 are both activated upon binding to cyclin K to regulate transcription through phosphorylating Ser2 residues located on the C-terminal domain (CTD) of RNA-polymerase II (RNA-Pol2) which contains 52 repeats of the YSPTSPS motif[6]. Selective inhibition of CDK12 kinase activity preferentially downregulates a small set of genes that respond to and mediate the repair of DNA-damage including homologous recombination (HR) repair genes BRAC1 and BRCA2[7, 8].

Inhibitors of CDK12 increase DNA-damage and have been demonstrated to potentiate the anti-proliferative effects of poly (ADP-ribose) polymerase (PARP) inhibitors[9]. Recently, an *in vivo* combination treatment of Dinaciclib (**Figure 1**), a clinical-stage non-selective CDK12 inhibitor, with Olaparib, a poly (ADP-ribose) polymerase (PARP) inhibitor, has demonstrated a significant tumor growth inhibition in a PDX ovarian model[10], spurring a wave of medicinal chemistry efforts to discover more potent and selective CDK12 inhibitors.

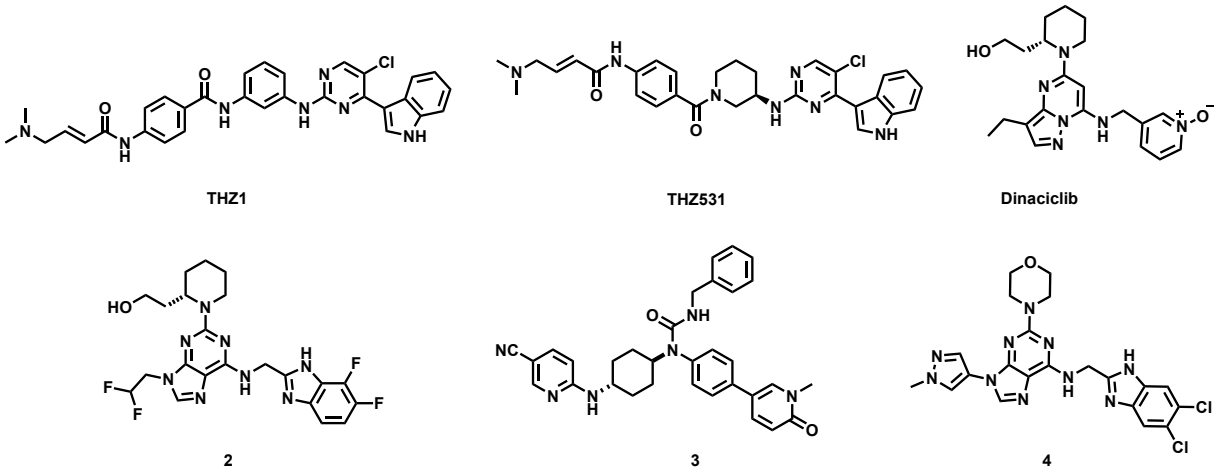

Figure 1. Structure of THZ1, THZ531, Dinaciclib and reported CDK12 inhibitors **2** to **4**

Amongst the reported inhibitors of CDK12 and CDK13 are the acrylamide-modified covalent inhibitors: THZ1 and THZ531 (**Figure 1**) in cancer cells, THZ531 was shown to irreversibly inhibit phosphorylation of ser2 of RNA pol II CTD, represses transcription of DNA damage response (DDR) genes and results in potent anti-proliferative effects[5]. Although validated as a cellular probe, THZ531 is not suitable for *in vivo* murine efficacy studies due to its poor metabolic stability resulting in high clearance in mice[5]. In addition to the covalent inhibitors, Dinaciclib[11], a clinical-stage pan-CDK inhibitor, exhibits activity in numerous models but is not suitable as a selective pharmacological probe of CDK12.

Recently, 2,6,9-trisubstituted purines (**2** and **4**) and a trisubstituted urea (**3**, **Figure 1**) have been reported as reversible CDK12 inhibitors that exhibit high kinase selectivity for CDK12[12-14]. Here we report our efforts that culminated in the development of MFH290, a highly-selective covalent inhibitor of CDK12/13 using a structure-guided drug design strategy by combining structural features of THZ531 with a previously reported non-covalent, pan-CDK inhibitor SNS032[15] (**Figure 2A**).

CHEMISTRY

The synthesis of compounds **1a**, **1b** and **1c** is depicted in **Scheme 1**. Commercially available intermediate **4a** reacts with carboxylic acids **5**, **6** or **7** through a HATU-mediated condensation reaction under basic conditions to provide the final compound **1a** or the intermediate **8** and **9** after deprotection of the Boc group. While **8** was then subjected to a second amide condensation reaction with 3-acrylamidobenzoic acid **5** to afford **1b**, compound **9** was treated with acryloyl chloride under basic conditions to introduce the acrylamide warhead to generate **1c**.

Scheme 1. Synthesis of compounds 1a-c

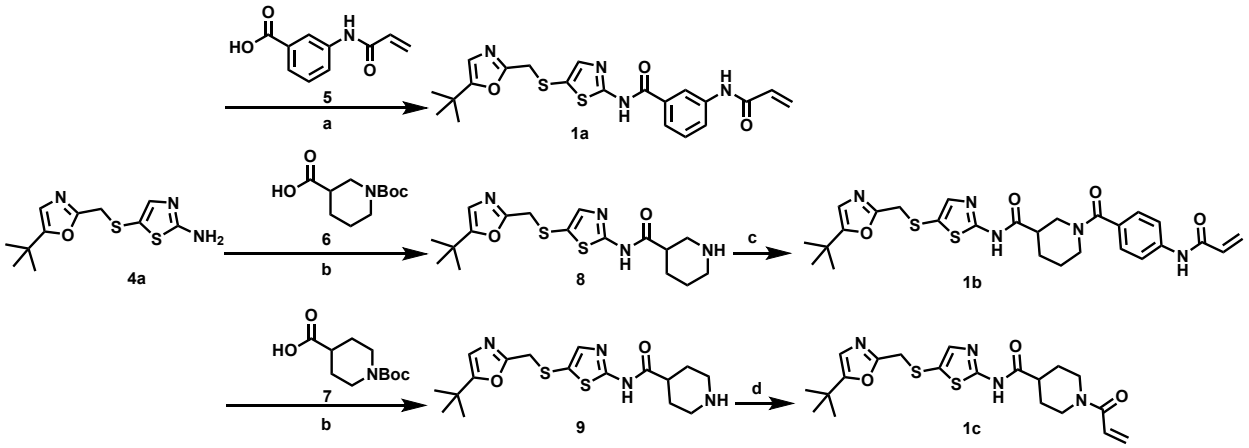

Reagents and conditions: (a) HATU, DIEA, DMF, 8%; (b) (i) DMAP, EDCI, triethylamine, DCM/DMF; (ii) TFA, DCM, 16-83%; (c) HATU, 4-acrylamidobenzoic acid, DIEA, DMF, 12%; (d) Acryloyl chloride, DIEA, THF, 0 ^{o}C, 51%.

Further analogs including **1d-1i, 1k** and **1l** were synthesized by reacting 2-(((2-bromothiazol-5-yl)thio)methyl)-5-(tert-butyl)oxazole (**10**) with Boc protected-3-amino piperidine or its variants or with 1,3-cyclohexane diamine to provide the intermediate **11** (**Scheme 2**). Free amino compound, derived from intermediate **11** after deprotection, was subjected to either a one-step amide coupling reaction with compound **12** or a three-step reaction as amide coupling (compound **13**), reduction (compound **14**) and acrylamide formation with acryl chloride, leading to the final products **1d-1i**, **1k** and **1l**.

Scheme 2. Synthesis of compounds 1d-1i, 1k and 1l.

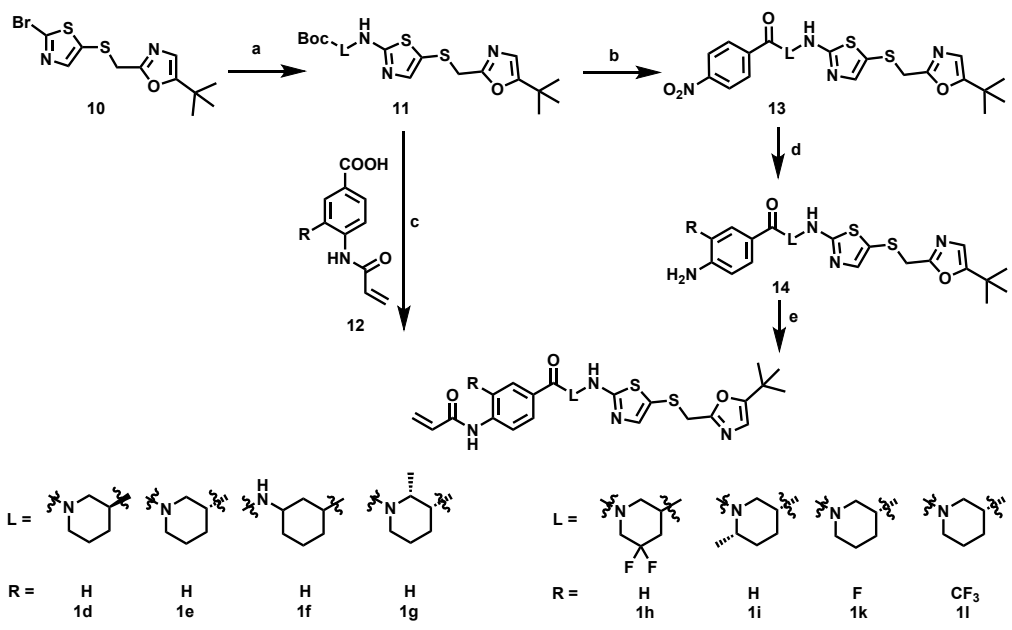

Reagents and conditions: (a) NMP, DIEA, 140 ^{o}C, 6-67%; (b) (i) 4N HCl/dioxane, MeOH, (ii) 4-nitrobenzoyl chloride, Py, 27-55%; (c) (i) 4N HCl/dioxane, MeOH, (ii) T_3P, DIEA,

DCM, 19-60%; (d) $SnCl_2$, ethyl acetate/MeOH, 80 °C, 24-76%; (e) acryloyl chloride, DIEA, MeCN, 0 °C, 16-41%.

Scheme 3. Synthesis of compounds 1j, 1m-1o and 1u-1v

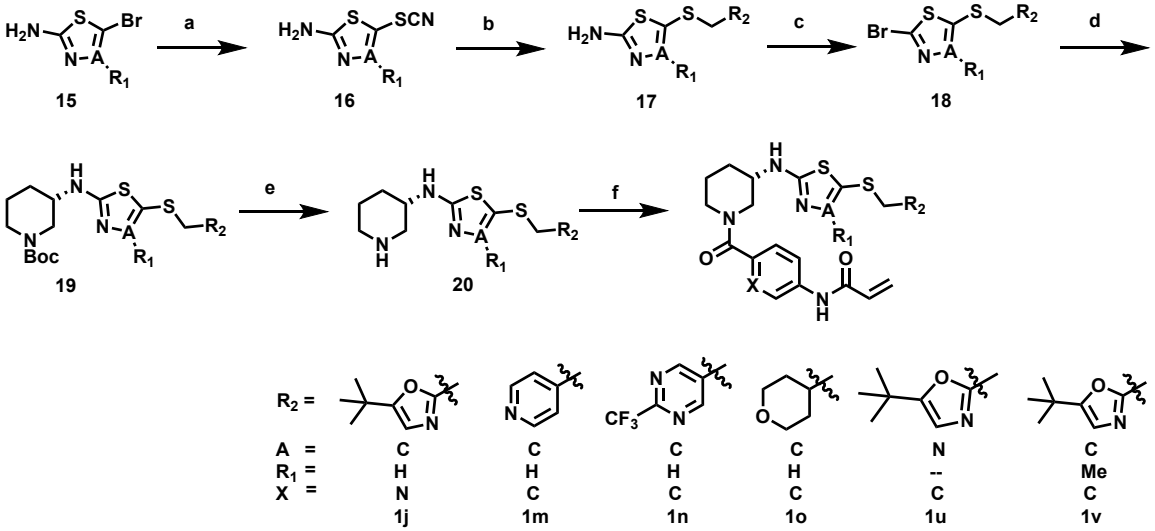

Reagents and conditions: (a) KSCN, MeOH, 41-93%; (b) (i) $NaBH_4$, ethanol, 0 °C to room temperature, (ii) R_2CH_2X, ethanol, 65 °C, 41-57%; (c) $CuBr_2$, *t*-BuONO, MeCN, 0 °C, 37-94%; (d) 1-Boc-(*R*)-3-aminopiperidine, NMP, DIEA, 140 °C, 53-67%; (e) 4N HCl/dioxane, MeOH, 51-95% ; (f) 4-acrylamidobenzoic acid, T_3P, DIEA, DCM, 53% or (i) benzoyl chloride, Py or benzoic acid, HATU, DIEA, DMF, (ii) $SnCl_2$, ethyl acetate/MeOH, 80 °C, (iii) acryloyl chloride, DIEA, MeCN, 0 °C, 7-17%.

Scheme 3 presents the strategy to synthesize compounds **1j**, **1m-1o** and **1u-1v**. The commercially available starting material: 2,4,5-trisubstituted thiazole, or 2,5-disubstituted thiadiazole were reacted with KSCN to afford thiocyanate intermediate **16**. In a one-pot reaction thiocyanate **16** was reduced to corresponding thiol using $NaBH_4$, and then alkylated with the appropriate halide. The intermediate **17** was subjected to Sandmeyer reaction to convert the amine group to the bromide, which was then replace by a Boc-

protected-3-amino-piperidine. Deprotection of Boc from intermediate **19** led to compound **20**, which was then processed using the same procedure as shown in **Scheme 2** to generate the final products. The compound **1t** was synthesized with a similar reaction route with 2,4,5-trichloropyrimidine as the starting material shown in **Scheme 4**.

Scheme 4. Synthesis of compound 1t

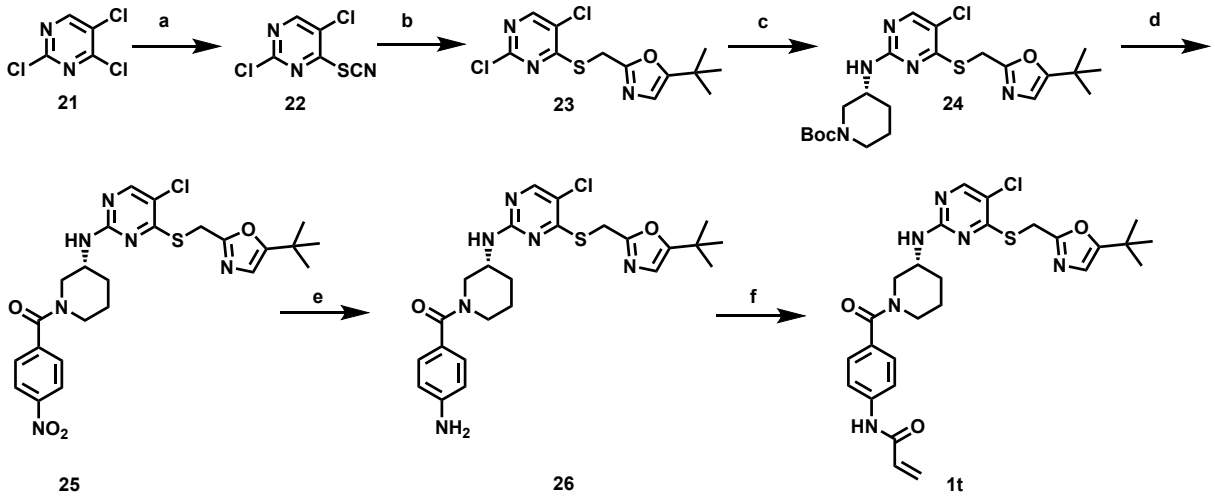

Reagents and conditions: (a) KSCN, MeOH, 55%; (b) (i) NaBH4, ethanol, 0 ^{o}C to RT, (ii) 5-(tert-butyl)-2-(chloromethyl)oxazole, ethanol, 65 ^{o}C, 17%; (c) 1-Boc-(*R*)-3-aminopiperidine, NMP, DIEA, 140 ^{o}C, 92%; (d) (i) 4N HCl/dioxane, MeOH, (ii) 4-nitrobenzoyl chloride, Py, 89%; (e) $SnCl_2$, ethyl acetate/MeOH, 80 ^{o}C, 20%; (f) acryloyl chloride, DIEA, MeCN, 0 ^{o}C, 65%.

The synthesis of compound **1p**, **1q** and **1r** that contain different linkers between the oxazole and thiazolyl ring was carried out as shown in **Scheme 5** and **6**. First, the Wittig reaction was performed using aldehyde **29** and phosphonate intermediate **28**, prepared from 5-(tert-butyl)-2-(chloromethyl)oxazole using an Arbuzov reaction. Reduction of the double bond with hydrogen/Pd provided intermediate **31**, which was converted to

compound **32** by a Sandmeyer reaction. Installation of piperidine and acrylamide warhead was followed by the same procedure as shown in **Scheme 2**.

Scheme 5. Synthesis of compound 1p

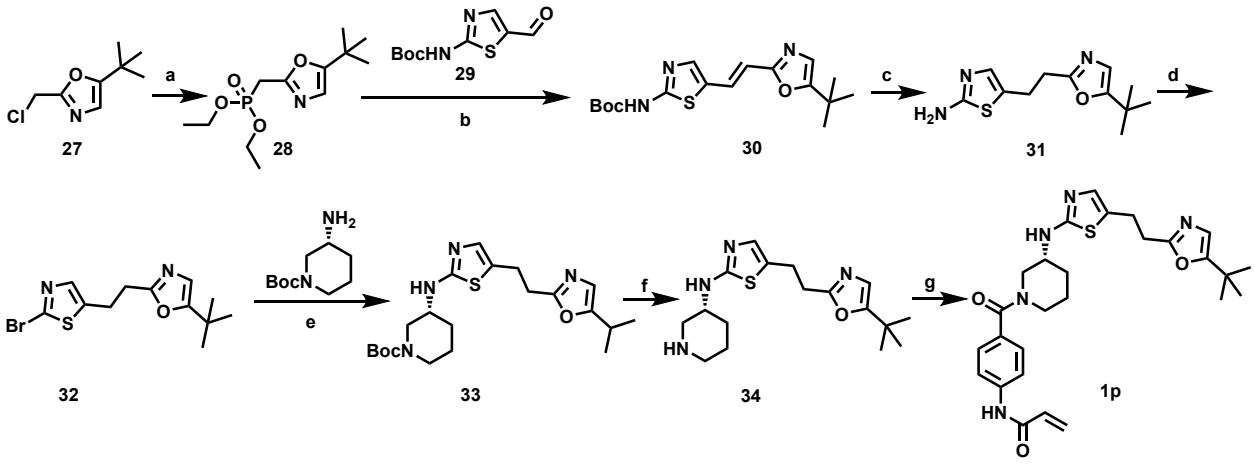

Reagents and conditions: (a) triethyl phosphite, 120 °C, 39%; (b) *t*-BuOK, THF, 84%; (c) H_2, Pd/C, MeOH, then 4N HCl/dioxane, 90%; (d) $CuBr_2$, *t*-BuONO, MeCN, 0 °C, 53%; (e) NMP, DIEA, 140 °C, 63%; (f) 4N HCl/dioxane, MeOH, 88%; (g) 4-acrylamidobenzoic acid, HOBT, EDCI, DIEA, DMF, 16%.

For **1q** and **1r**, the synthesis of **36** is straightforward as **35** and **27** are all commercially available reagents and thus one-step substitution reaction led to the key intermediate **41a**. Intermediate **41b** was synthesized using a 3-step reaction sequence involving coupling 2-bromothiazole-5-carbonitrile with 3-aminopiperidine followed by reduction of cyano group to a primary amine and further reaction with 5-(tert-butyl)-2-(chloromethyl)oxazole. The rest of reactions to install the acrylamide is same as shown in **Scheme 2**.

Scheme 6. Synthesis of compounds 1q and 1r

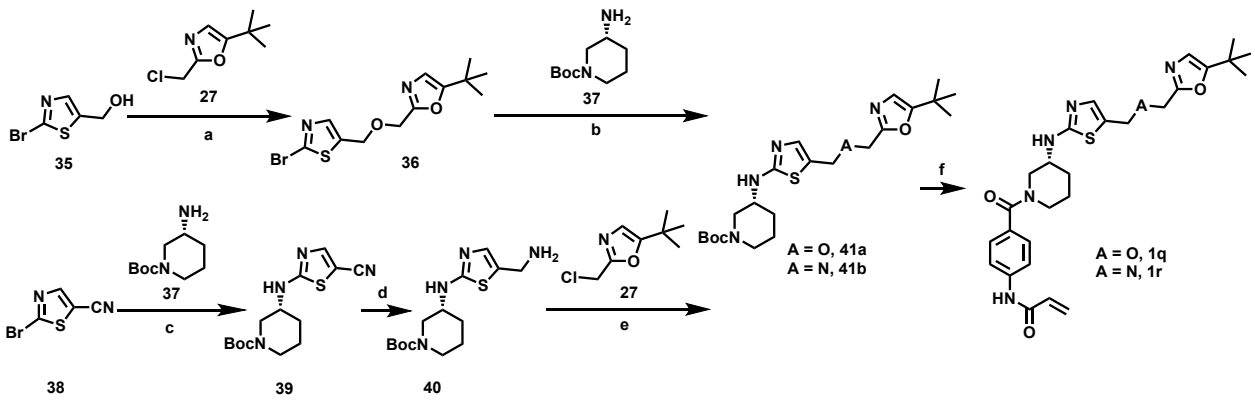

Reagents and conditions: (a) NaOH, DMF, 120 ^{o}C, 45%; (b) NMP, DIEA, 140 ^{o}C, 22%; (c) THF, DIEA, 80 ^{o}C, 97%; (d) $CoCl_2$-$6H_2O$, $NaBH_4$, ethanol, 28%; (e) NMP, DIEA, 80 ^{o}C, 58%; (f) (i) 4N HCl/dioxane, MeOH, (ii) 4-acrylamidobenzoic acid, HOBT, EDCI, DIEA, DMF, 22-38%.

RESULT

Development of MFH290 as covalent CDK12 inhibitor

High-throughput biochemical screening of kinase-focused chemical libraries is a common method to find starting points for inhibitor optimization campaigns. However our efforts to develop a kinase assay suitable for screening CDK12 reversible inhibitors were unsuccessful. Therefore, we changed our strategy to use a competition-based pull-down assay to screen for reversible CDK12 binders. Our aim was to identify compounds that bound CDK12 that could be optimized and converted to covalent inhibitors targeting the uniquely positioned cysteine 1039 (Cys1039) residue that lies in the C-terminal domain of CDK12. Competitive pull-down assays were performed by utilizing biotinylated (bio)THZ1, which has been shown to covalently bind and pulldown both CDK12 and CDK13 (CDK12/13)[5]. As bioTHZ1 can be pulled down using streptavidin-coated beads, we gauged the ability of bioTHZ1 to bind free CDK12/13 by monitoring the extent to which

CDK12, CDK13, or their obligate binding partner, cyclin K, were pulled down. We screened a focused collection of reported CDK inhibitors for their ability to protect CDK12 and 13 from being pulled down by bioTHZ1 (**Supplementary figure S1A**). Amongst all known CDK inhibitors we screened, pretreatment with SNS032, a known inhibitor of CDK2, 7 and 9 (**Figure 2A**), resulted in a significant reduction of cyclin K pulldown from Jurkat cells by bioTHZ1 (**Supplementary figure S1B**), providing a starting point for medicinal chemistry efforts.

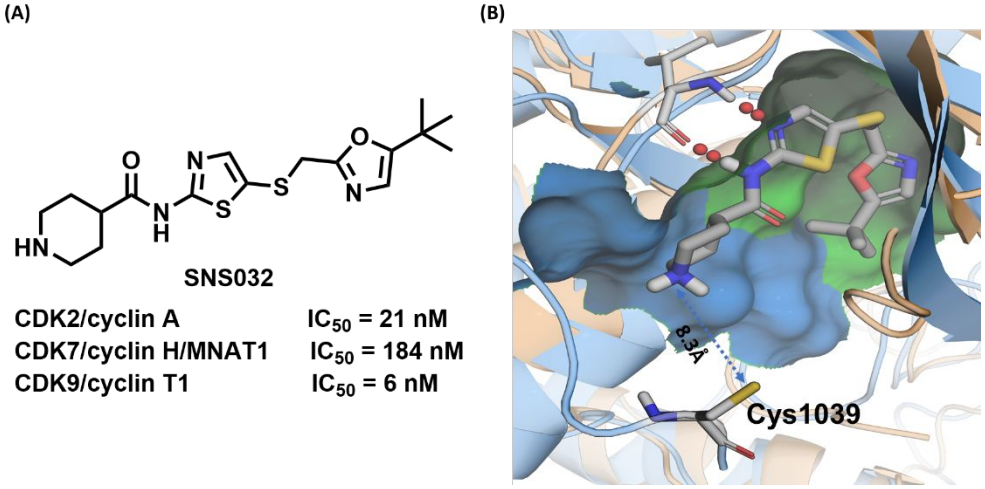

Figure 2. (A) Structure and biochemical IC_{50} of SNS032 (B) Overlay of SNS032/CDK2 (PDB code: 5D1J, beige) and CDK12 (PDB code: 5ACB, blue) reveals that the piperidine ring could be extended towards Cys1039.

The co-crystal structure of SNS032 with CDK2 (PDB: 5D1J) clearly illustrates the binding mode where the: (1) 3-aminothiazole group forms two key hydrogen bonds with the hinge region; (2) 5-(tert-butyl)oxazole ring occupies the back hydrophobic pocket II; and (3) the piperidine faces the solvent exposed region. Structural overlay of CDK12 crystal structure (PDB: 5ACB) and SNS032/CDK2 co-crystal structure indicated that the solvent-exposed

piperidine ring would lie in close proximity to Cys1039 (**Figure 2B**). Subsequent chemistry was performed to explore the ability to form a covalent bond with Cys1039 and to gain additional selectivity for CDK12 relative to other kinases. All newly synthesized compounds were assayed for CDK12 binding using the bioTHZ1 competition assay **Supplementary figure S2)**. To quickly assess the selectivity for CDK12 versus the other CDKs targeted by SNS032, we used commercially available biochemical assays from Life Technologies for CDK2/Cyclin A, CDK7/Cyclin H/MNAT1 and CDK9/Cyclin T1. In addition, we engineered HAP1 cells by mutating Cys1039 of CDK12 to a non-reactive serine to generate a chemical-genetic system to allow dissection of covalent-dependent inhibitor pharmacology.

To explore advantageous modifications to SNS032 we started by installing the requisite acrylamide warhead on the solvent exposed region facing the cysteine residue. For example, compounds **1a**, **1b** and **1c** were all designed with an acrylamide group attached to either phenyl or piperidine ring which structural alignment suggested would position this warhead in close proximity to Cys1039. All warhead modifications conserved the ability to block cyclin K pulldown with bioTHZ1, indicating that CDK12/13 binding was preserved (**Table 1**). In regard to selectivity, compound **1b** maintained inhibitory activity against all the CDKs tested, whereas **1a** and **1c** exhibited dramatically reduced inhibition of CDK7 （**Table 1** and **Supplementary figure S2**）. In contrast, 3-aminopiperidine, which based on our work on THZ531 emerged as a privileged scaffold for selective CDK12 inhibition, led to a dramatic reduction in inhibition of CDK2/7/9 activity while CDK12/13 binding was retained (**1d**, hereafter named MFH290, **Table 1**). Moreover, the S-enantiomer of MFH290 (**1e**) lost the ability to target CDK12, meaning that R

configuration of 3-aminopiperidine is required to provide the proper trajectory to target Cys1039. Removing the carbonyl and installing an amino group through 3-amino-cyclohexane (**1f**) slightly reduced CDK12 binding while also significantly restoring activity on CDK2 and CDK9. Therefore, further modifications focused on retaining the 3-aminopiperidine moiety.

Introduction of either a methyl group to the 2-position (**1g**), or two fluorines to 5-postion of piperidine ring (**1h**), abrogated the inhibitory activity on all CDKs, whereas introduction of a methyl group to the 6-position (**1i**) resulted in comparable, but less selective, activity to MFH290. Moreover, a phenyl ring extending from the piperidine was found to be more favored than a pyridine ring (**1j**) and a small group such as a fluorine (**1k**) was better tolerated compared to a larger CF_3 group at the 4-position (**1l**) (**Table 1**). Replacement of the tert-butyloxazole group with pyridine (**1m**), pyrimidine (**1n**), or tetrahydropyran (**1o**) rings resulted in compete loss of activity. Additionally, the thioether linkage to the core thiazole was necessary for CDK12/13 activity as all non-thioether linked compounds such as **1p**, **1q** and **1r** were inactive (**Table 2**). Likewise, oxidation of the thiol to sulfoxide (**1s**) diminished inhibition and binding to CDK2/7/9 and CDK12. Finally, a non-substituted thiazole core was most favored as replacement with a pyrimidine (**1t**), thiadiazole (**1u**), or even methylated thiazole (**1v**) significantly reduced CDK12 binding activity (**Table 3**). Taken all together, MFH290 emerged as our best-in-class inhibitor from this series.

Table 1. IC_{50} value or pulldown competition percentage with bioTHZ1 of compounds SNS032, 1a-1l against CDK2,7,9 and CDK12

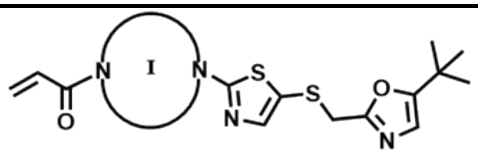

Compound	I	IC$_{50}$ (nM)			CDK12[c]
		CDK2[a]	CDK7[b]	CDK9[b]	(percentage)
SNS032	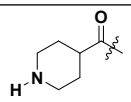	21	184	6	34.6
1a	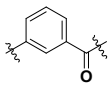	58.8	1140	24.6	0.3
1b	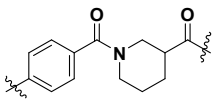	11	99	1.79	0.3
1c	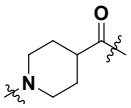	10.8	457	3.16	2.6
1d[e]	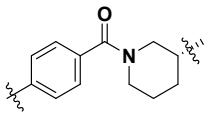	120	6020	114	0
1e	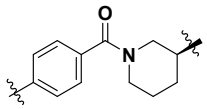	>10000	>10000	>10000	78.2
1f	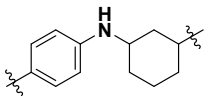	15.7	557	30.9	0.8

1g	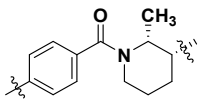	1420	7790	257	3.1
1h	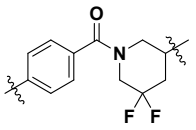	1480	9600	1100	3.5
1i	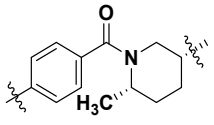	73.2	609	14.7	0.1
1j	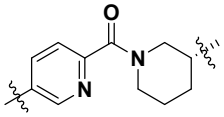	561	3890	514	1.2
1k	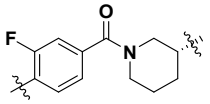	211	5540	138	0
1l	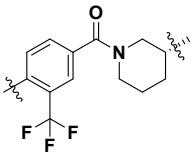	142	3490	87.6	1.0

[a] tested using Z'-Lyte assays with ATP concentrations at the apparent K_M.

[b] tested using Adapta assays with ATP concentrations at the apparent K_M.

[c] tested using CDK12 pulldown assay. The remaining CDK12 protein in the presence of each compound was pulled down using bioTHZ1, and quantified by densitometry of the bands of CDK12 (normalized with DMSO-treated).

[e] "**1d**" is MFH290.

Table 2. IC_{50} value or pulldown competition percentage with bioTHZ1 of 1m-1s against CDK2, 7,9 and CDK12

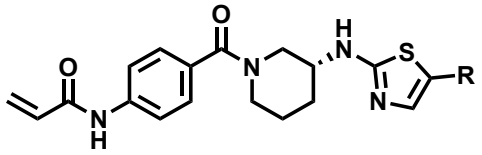

Compound	R	IC$_{50}$ (nM)			CDK12[c]
		CDK2[a]	CDK7[b]	CDK9[b]	(percentage)
1m	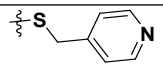	>10000	>10000	>10000	100
1n	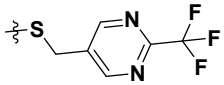	>10000	>10000	>10000	74.1
1o	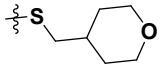	>10000	>10000	>10000	100
1p	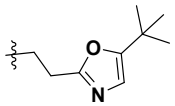	>10000	>10000	>10000	41.0
1q	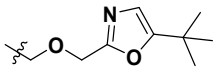	>10000	>10000	>10000	81.4
1r	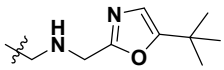	3170	8870	7140	81.3
1s	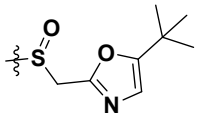	>10000	>10000	9220	85.7

[a, b, c] defined in Table 1

Table 3. IC$_{50}$ value or pulldown competition percentage with bioTHZ1 of compounds1t-1v against CDK2, 7,9 and CDK12

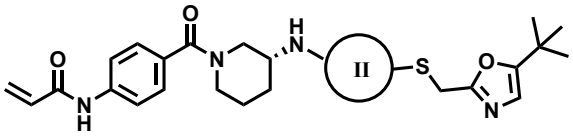

Compound	II	IC_{50} (nM)			CDK12[c]
		CDK2[a]	CDK7[b]	CDK9[b]	(percentage)
1t	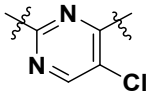	>10000	5120	>10000	5.4
1u	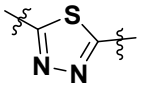	>10000	>10000	>10000	100
1v	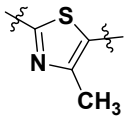	>10000	>10000	2870	91.2

[a, b, c] defined in Table 1

To confirm the covalent bond formation of MFH290 with Cys1039 on CDK12, we analyzed purified CDK12 protein by LC-MS after incubation with a 10-fold molar excess of MFH290 for 2 hours at 37 °C, and observed a mass shift consistent with addition of a single molecule of MFH290 to CDK12 (**Figure 3A** and **3B**). To confirm the site of modification, labeled protein was digested with trypsin, and peptides analyzed by capillary electrophoresis-MS/MS. Database search revealed exclusive modification of CDK12 by MFH290 at Cys1039 (**Figure 3C**). Taken together, our mass spectrometry-based analysis showed that MFH290 forms a covalent adduct with CDK12 by reacting with a single cysteine, Cys1039. We therefore carried MFH290 forward into all subsequent cellular experiments to characterize the inhibitor and evaluate CDK12/13 function.

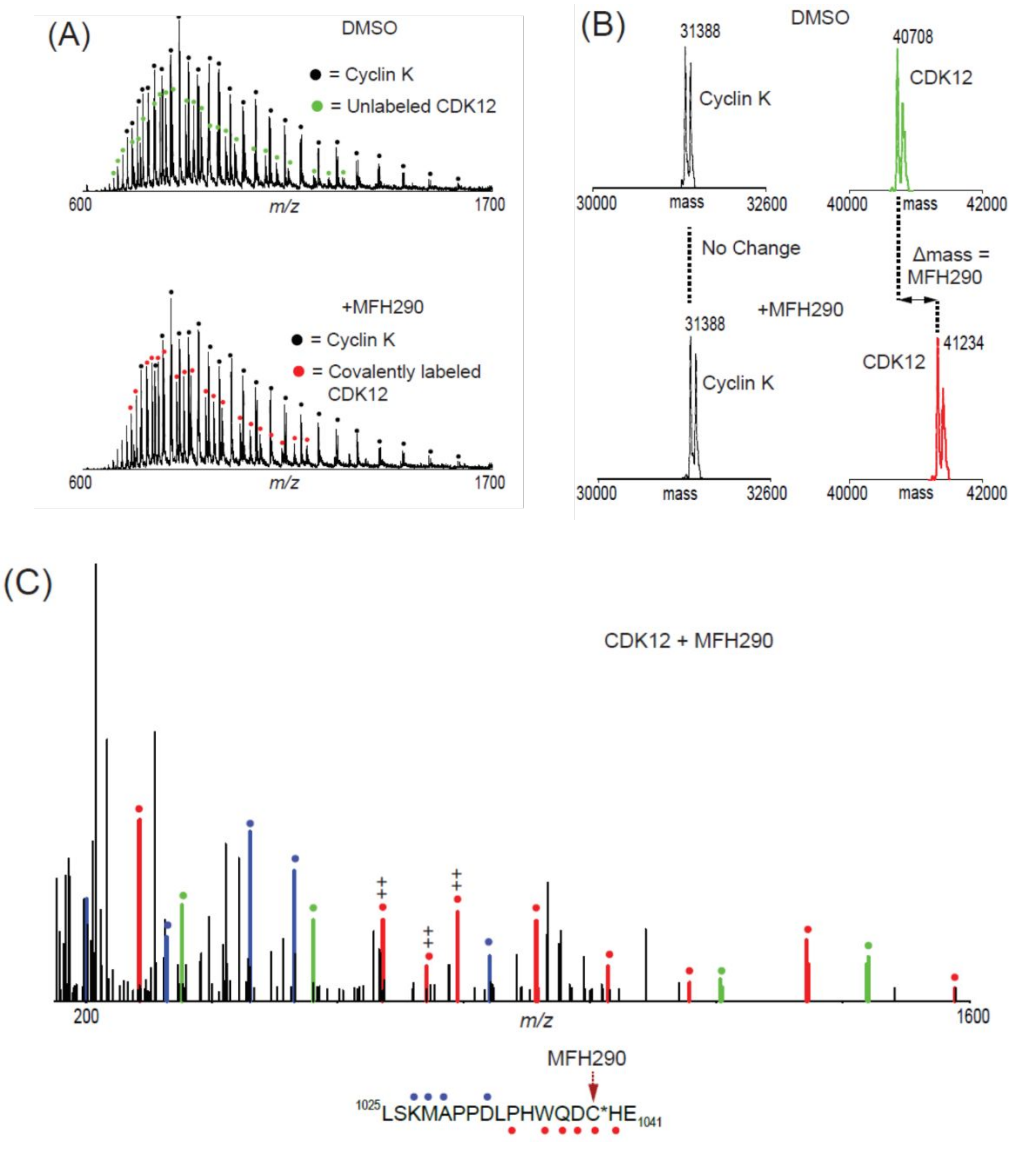

Figure 3. CDK12 is exclusively labeled by MFH290 at Cys1039. (A) Mass spectra and (B) zero-charge mass spectra of CDK12/Cyclin K complex treated with (top) DMSO or (bottom) a 10-fold excess of MFH290 for 1 hour at room temperature. (A) Mass spectral peaks corresponding to Cyclin K, unmodified CDK12, and CDK12 covalently labeled with MFH290 are indicated with black, green, or red circles, respectively. (B, left) Cyclin K is unaffected by compound treatment while (B, right) CDK12 protein exhibits an increase in mass consistent with modification by a single molecule of MFH290. (C) MS/MS spectrum

of CDK12 peptide ^{1025}LSKMAPPDLPHWQDC HE$_{1041}$ modified with MFH290 indicates covalent labeling of Cys1039. Ions of type b and y are indicated with blue and red glyphs respectively. Inhibitor related ions 1^{16} are marked with green glyphs.

To characterize the kinome-wide selectivity of MFH290, we employed DiscoverX's KinomeScan binding assays against a panel of 468 kinases at a concentration of 1 μM[17, 18]. As shown in **Figure 4A** and **Supplementary table S1**, MFH290 exhibits exquisite selectivity with CDK13 as the only potently inhibited target (CDK12 is not included in the panel). We also tested MFH290 on an extensive enzymatic CDKs panel which included CDKs 1-9, 12-14 and 16. The measured IC$_{50}$s across all other CDKs are higher than 100 nM, indicating that MFH290 did not potently inhibit any of these CDKs (**Figure 4B**).

(A)

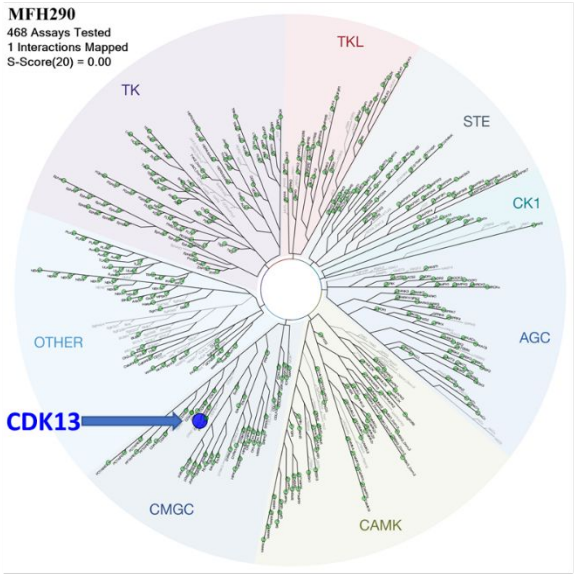

(B)

CDKs	IC$_{50}$ (nM)
CDK1[a]	1470
CDK2[a]	120
CDK3[b]	366
CDK4[c]	>10000
CDK5[a]	1130
CDK6[c]	>10000
CDK7[c]	6020
CDK8[b]	4490
CDK9[c]	114
CDK12[d]	25
CDK13[d]	49
CDK14[b]	3130
CDK16[b]	3830

Figure 4. (A) Kinase profiling of MFH290. The levels of binding were measured at concentrations 1 μM against a panel of 468 human kinases. The results for the binding interactions are reported as blue circles in the KiNOME tree. (B) IC$_{50}$ values for MFH290

against CDK1-9, 12-14 and 16. [a] tested in Z'-Lyte assays with ATP concentrations of K_M. [b] tested in LanthaScreen™ Eu Kinase Binding Assay with ATP concentrations of K_M. [c] tested using Adapta assays with ATP concentrations at the apparent K_M. [d] tested in radioisotope filter binding assay.

To define the working concentration range of MFH290, we employed the same competition-based target engagement assay described above (**Supplementary figure S1A**). Concentrations of MFH290 that block bioTHZ1-mediated pulldown of CDK12/13/cyclin K identify doses at which MFH290 covalently binds CDK12/13 in cells. Experiments in both Jurkat T-ALL and HAP1 (a near haploid) CML lines indicate that MFH290 saturates CDK12/13 binding at a concentration of approximately 40 nM (**Figure 5A**, **Supplementary figure S3**).

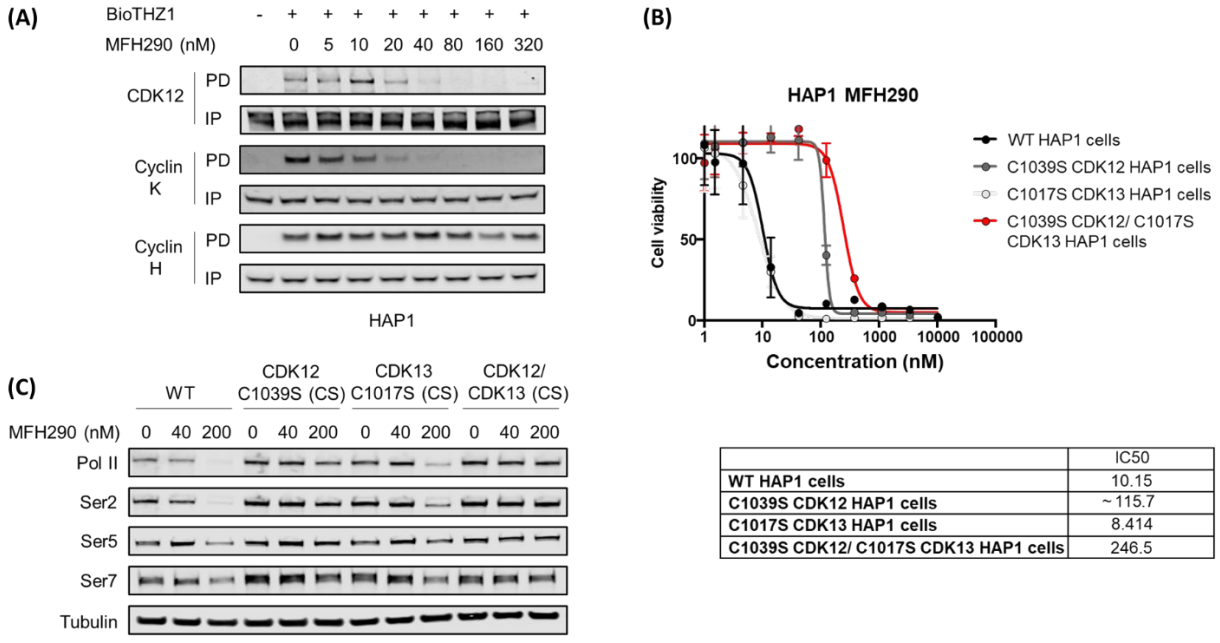

	IC50
WT HAP1 cells	10.15
C1039S CDK12 HAP1 cells	~ 115.7
C1017S CDK13 HAP1 cells	8.414
C1039S CDK12/ C1017S CDK13 HAP1 cells	246.5

Figure 5. (A) MFH290 targets CDK12 and CDK13 in cells. Treatment of HAP1 cells with MFH290 for 6 hours blocks pull down of CDK12 and associated cyclin K by biotinylated

THZ1. **(B)** Antiproliferation assay using WT, CDK12 C1039S, CDK13 C1017S, and CDK12 C1039S/ CDK13 C1017S doubly-mutated HAP1 cells. Output is CellTiterGlo® luminescent signal following 72-hour treatment with MFH290. **(C)** MFH290 reduces Pol II CTD phosphorylation in a concentration-dependent manner. Shown are effects of MFH290 on CTD phosphorylation in WT, CDK12 C1039S, CDK13 C1017S, and CDK12 C1039S/ CDK13 C1017S doubly-mutated HAP1 cells after 6 hours of treatment.

To determine the cellular selectivity of MFH290, we used CRISPR/Cas9-mediated allelic replacement[8] to establish isogenic cell lines expressing covalent inhibitor refractory cysteine-to-serine mutant forms of CDK12 (C1039S), CDK13 (C1017S), and CDK12/CDK13 double mutants (**Supplementary figure S4A**). These isogenic lines enable us to assess the relative contribution of CDK12, CDK13, and CDK12/13 inhibition to MFH290 pharmacology. Western blotting demonstrated that WT and mutant forms of CDK12 and CDK13 were all expressed at similar levels (**Supplementary figure S4B**).

We previously reported that THZ531, our first-generation CDK12/13 inhibitor, led to a pronounced and rapid decrease in cell proliferation[5], therefore we tested MFH290 across its effective dose range for antiproliferative activity in the HAP1 isogenic lines. In WT HAP1 cells, MFH290 displayed low nanomolar anti-proliferative activity. Mutation of the reactive cysteine within CDK12, but not CDK13, significantly blunted these effects, with CDK12 mutant cells exhibiting 11-fold resistance to MFH290 to WT CDK12 cells, which was further enhanced to 25-fold as compared to WT when both CDK12 and CDK13 were mutated (**Figure 5B**).

CDK12 and CDK13 have been implicated in the regulation of RNA polymerase II (Pol II)-mediated gene transcription by phosphorylating Pol II at conserved residues within the CTD[19]. Therefore, we asked whether MFH290 affected Pol II CTD phosphorylation levels in our HAP1 isogenic lines. Indeed, MFH290 treatment reduced Pol II CTD phosphorylation at serine residues 2, 5, 7 (Ser2, Ser5, Ser7), as well as overall Pol II levels (**Figure 5C**). Mutation of CDK12 greatly restored levels of both total and phosphorylated Pol II to near WT levels in the presence of MFH290, while mutation of CDK13 exhibited a significantly reduced rescue. Complete rescue of Pol II CTD phosphorylation was achieved by expressing both mutant CDK12 and CDK13 in HAP1 cells (**Figure 5C**). The difference in rescue demonstrated by mutation of CDK12 compared to that of CDK13 likely stems from the fact that CDK12 is the more highly expressed and predominant homolog in HAP1 cells.

As CDK12 has been shown to specifically regulate the expression of DNA damage response (DDR) genes[20], we treated HAP1 cells with MFH290 at 40 and 200 nM and analyzed expression of DDR RNA and protein expression by RT qPCR and western blot. We found that treatment with MFH290 reduced expression of *RAD51* and *RAD51C* at both the RNA and protein level (**Figure 6A** and **6B**). These effects were almost completely rescued at the protein level and largely rescued at the RNA level by expression of mutant CDK12 alone, or in combination with C1017S CDK13.

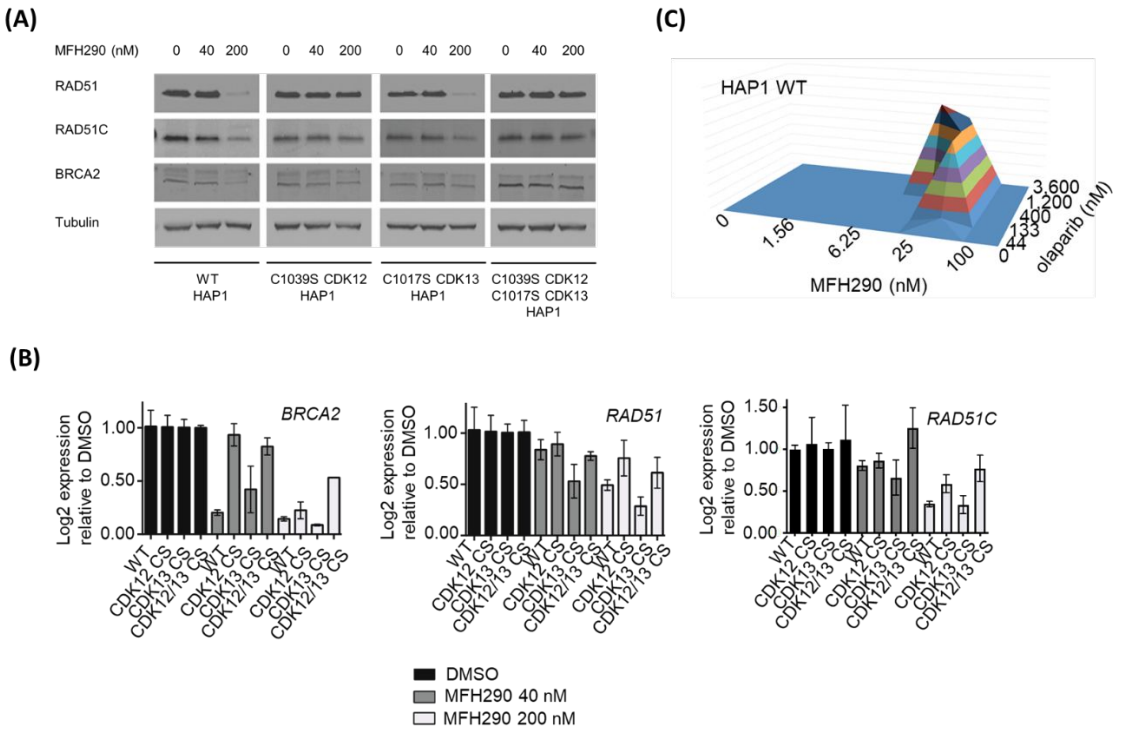

Figure 6. (A) MFH290 treatment leads to a reduction in DNA damage response proteins. Western blots of WT, CDK12 C1039S, CDK13 C1017S, and CDK12 C1039S/ CDK13 C1017S doubly-mutated HAP1 cells following treatment with MFH290 for 24 hours. (B) MFH290 treatment leads to reduced expression of DNA damage response genes. RT-qPCR of WT, CDK12 C1039S, CDK13 C1017S, and CDK12 C1039S/ CDK13 C1017S doubly-mutated HAP1 cells following treatment with MFH290 for 6 hours. (C) Excess over Bliss synergy plots for serial dilutions of MFH290 in combination with olaparib in HAP1 cells. Excess over Bliss scores > 0 indicate drug synergy, whereas negative scores indicate antagonism.

Impaired expression of RAD51 and other homologous recombination (HR)-regulating proteins have been shown to sensitize cancer cells to PARP inhibitors[21]. To ask if MFH290 could do the same, we treated HAP1 cells with increasing concentrations of both Olaparib, an FDA-approved PARP inhibitor, and MFH290. We examined the proliferation

data for synergistic effects as evaluated by extrapolated Excess over Bliss score (0-1)[22, 23]. Indeed MFH290 (25 nM) exhibited maximum synergy with Olaparib (1.2 μM) with excess over Bliss scores = 0.75 (**Figure 6C**).

These data indicate that CDK12 is the primary target of MFH290 in HAP1 cells, that covalent targeting of CDK12 is obligatory for MFH290 activity, and that CDK12 inhibition is largely responsible for the observed anti-proliferative effects. Consistent with biochemical kinase profiling, these results indicate that MFH290 has exceptional cellular selectivity for CDK12/13 (**Table 1-3**), supporting the notion that CDK12/13 inhibition is responsible for inhibitor-induced effects on DDR gene expression.

In order to know whether MFH290 is suitable for an in vivo efficacy study, we then took the compound for a pharmacokinetic study. As shown in the **Table 4**， MFH290 showed a short half-life in mouse plasma and a high clearance, indicating further optimization will be needed to improve its *in vivo* stability.

Table 4. Pharmacokinetic Parameters of MFH290

Route	Dose	T_{max}	$^{a}C_0/C_{max}$	AUC_{last}	$T_{1/2}$	CL	V_{ss}	F^{b}
	(mg/kg)	(hr)	(ng/mL)	(hr*ng/mL)	(hr)	(mL/min/kg)	(mL/kg)	(%)
i.v.	1	-	1312.89	162.22	0.17	102.03	730	-
i.p.	5	0.08	885.05	393.63	0.15	-	-	49
p.o.	10	0.25	556.46	412.44	-	-	-	25

a - **C_0**, back extrapolated conc. for i.v. group

b - **AUC_{last}** was considered for calculating bioavailability

Discussion and Conclusions

In conclusion, we have converted a pan-CDK inhibitor SNS032 to a selective CDK12/13 inhibitor MFH290 by hybridizing it with structural elements of the first selective CDK12/13 covalent inhibitor THZ531. Extensive structure-guided medicinal chemistry modifications delivered a narrow SAR, with (*R*)-3-aminopiperidine emerging as a privileged scaffold, enabling high binding affinity for CDK12/13 to the exclusion of other CDKs. MFH290 formed a covalent bond with Cys1039 on CDK12 and thus demonstrated a sustained CDK12 inhibition-induced phenotype including strong anti-proliferative effect on cancer cells, a transcriptional defect for DDR genes and a combinatorial effect with PARP inhibition. Compared to first generation covalent inhibitor THZ531, a higher degree of rescue from MFH290-induced phenotypes in HAP1 cells engineered with cysteine-to-serine CDK12 and CDK13 mutations, implies that MFH290 possesses a superior selectivity for CDK12/13. Further optimization of this scaffold to improve *in vivo* properties will enable *in vivo* investigation of drug efficacy.

EXPERIMENTAL SECTION

Chemistry.

Unless otherwise noted, reagents and solvents were obtained from commercial suppliers and were used without further purification. ^{1}H NMR spectra were recorded on 500 MHz (Bruker A500), and chemical shifts are reported in parts per million (ppm, δ) downfield from tetramethylsilane (TMS). Coupling constants (J) are reported in Hz. Spin multiplicities are described as s (singlet), br (broad singlet), d (doublet), t (triplet), q (quartet), and m (multiplet). Mass spectra were obtained on a Waters Micromass ZQ instrument. Preparative HPLC was performed on a Waters Sunfire C18 column (19 x 50

mm, 5μM) using a gradient of 15-95% methanol in water or acetonitrile in water containing 0.05% trifluoroacetic acid (TFA) over 22 min (28 min run time) or 35 min (45 min run time) at a flow rate of 20 mL/min. All of the final compounds reported had purities greater than 95% based on ^{1}H nuclear magnetic resonance (NMR) and liquid chromatography−mass spectrometry (LC−MS).

Synthesis of compound 1a.

To a solution of 5-(((5-(tert-butyl)oxazol-2-yl)methyl)thio)thiazol-2-amine (54 mg, 0.2 mmol) in DMF (1 mL) was added HATU (160 mg, 0.42 mmol), 3-acrylamidobenzoic acid (60 mg, 0.31mmol) and DIEA (52 mg, 0.4 mmol). The resulting mixture was stirred at room temperature for 1 hour, and then diluted with ethyl acetate (100 mL). The mixture was washed with water and brine, dried over Na_2SO_4 and concentrated. The residue was purified by silica gel column (MeOH/DCM, 0-15%) to afford the compound **1a** (7 mg, yield 8%) as a white solid.

*3-acrylamido-N-(5-(((5-(tert-butyl)oxazol-2-yl)methyl)thio)thiazol-2-yl)benzamide (**1a**).* ^{1}H NMR (400 MHz, $CDCl_3$) δ 12.36 (s, 1H), 9.08 (s, 1H), 8.24-7.99 (m, 1H), 7.90 (s, 1H), 7.63 (d, J = 7.6 Hz, 1H), 7.41 (t, J = 7.9 Hz, 1H), 6.95 (s, 1H), 6.55 (s, 1H), 6.44 (d, J = 16.8 Hz, 1H), 6.32 (dd, J = 16.8, 10.0 Hz, 1H), 5.76 (d, J = 10.0 Hz, 1H), 3.95 (s, 2H), 1.23 (s, 9H). MS (ESI) m/z 443.12 $[M+H]^+$.

Synthesis of compounds 1b and 1c.

To a solution of 5-(((5-(tert-butyl)oxazol-2-yl)methyl)thio)thiazol-2-amine (**4**) (0.69 mmol, 1 equiv), appropriate acid (0.94 mmol, 1.4 equiv), DMAP (0.35mmol, 0.5 equiv) and triethylamine (1.4 mmol, 2 equiv) in DMF (1 mL) and DCM (2 ml) was added EDCI (1.4

mmol, 2 equiv) at room temperature. The reaction mixture was stirred for 1.5 hour, and then diluted with ethyl acetate. The solution was washed with water and brine, dried over Na_2SO_4 and concentrated. The residue was purified by silica gel column and then treated with 4M HCl ethyl acetate (3mL). The reaction was stirred at room temperature for 30 min. The mixture was concentrated under vacuum to afford the compounds **8** and **9** as HCl salt.

To a solution of **8** (50 mg, 0.12 mmol) in DMF (1 mL) was added HATU (92 mg, 0.24 mmol), 4-acrylamidobenzoic acid (46 mg, 0.24 mmol) and DIEA (0.22 ml, 1.2 mmol). The resulting mixture was stirred at room temperature for 1 h, and then diluted with ethyl acetate (100 mL). The solution was washed with water and brine, dried over Na_2SO_4 and concentrated. The residue was purified by silica gel column (MeOH/DCM, 0-20%) to afford the compound **1b** as a white solid.

*1-(4-acrylamidobenzoyl)-N-(5-(((5-(tert-butyl)oxazol-2-yl)methyl)thio)thiazol-2-yl)piperidine-3-carboxamide (**1b**).* ^{1}H NMR (400 MHz, DMSO) δ 12.37 (s, 1H), 10.32 (s, 1H), 7.73 (d, J = 7.8 Hz, 2H), 7.55-7.22 (m, 3H), 6.71 (s, 1H), 6.44 (dd, J = 16.9, 10.3 Hz, 1H), 6.28 (d, J = 16.8 Hz, 1H), 5.78 (d, J = 9.9 Hz, 1H), 4.05 (s, 2H), 3.67-2.69 (m, 4H), 1.97-1.23 (m, 5H), 1.12 (s, 9H). MS (ESI) m/ 554.21 $[M+H]^+$.

To a solution of **9** (20 mg, 0.05 mmol) in THF (5 mL) was added DIEA (17 mg, 0.15 mmol) and acryloyl chloride (43 mg, 0.05 mmol) at 0 ^{o}C for 1 hour. The resulting mixture was stirred at room temperature for 2 hours. The solution was concentrated and purified by silica gel column (MeOH/DCM, 0-20%) to afford the compound **1c** as a slightly white solid.

*1-acryloyl-N-(5-(((5-(tert-butyl)oxazol-2-yl)methyl)thio)thiazol-2-yl)piperidine-4-carboxamide (**1c**).* ^{1}H NMR (400 MHz, $CDCl_3$) δ 11.64 (s, 1H), 7.29 (s, 1H), 6.61-6.55 (m,

2H), 6.28 (d, J = 16.7 Hz, 1H), 5.71 (d, J = 10.6 Hz, 1H), 4.60-4.57 (m, 1H), 4.12-3.96 (m, 1H), 3.96 (s, 2H), 3.21-2.90 (m, 2H), 2.68 (t, J = 10.4 Hz, 1H), 2.01-1.82 (m, 4H), 1.24 (s, 9H). MS (ESI) m/z 435.15 $[M+H]^+$.

Synthesis of compounds 1d-1f.

A mixture of 2-(((2-bromothiazol-5-yl)thio)methyl)-5-(tert-butyl)oxazole[24] (**10**) (0.45 mmol, 1 equiv), appropriate amine (0.9 mmol, 2 equiv) and DIEA (1.35 mmol, 3 equiv) in NMP (3 mL) was heated to 140 °C overnight. The solution was diluted with water (20 mL) and extracted with chloroform and iso-propanol (4:1). The organic phase was washed with brine (50 mL × 2) and dried over Na_2SO_4, filtered and concentrated. The residue was purified by silica gel column (MeOH/DCM, 0-20%) to give compound **11**.

To a mixture of **11** (0.33 mmol, 1 equiv) in methanol (2 mL) was added 4N HCl/dioxane (2 mL). The resulted solution was stirred at room temperature for 3 h. The mixture was concentrated under reduced pressure to give the corresponding HCl salt. To the solution of HCl salt (0.33 mmol, 1 equiv) in pyridine (2 mL) was added 4-nitrobenzoyl chloride (0.66 mmol, 2 equiv), the reaction mixture was stirred at room temperature overnight. The resulting mixture was concentrated under reduced pressure and the residue was purified by silica gel column (MeOH/DCM, 0-20%) to give compound **13**.

To a solution of **13** (0.54 mmol, 1 equiv) in ethyl acetate and methanol (1:1) were added Tin (II) chloride dehydrate (5.4 mmol, 10 equiv) and conc. HCl (0.2 mL). After stirring for 3 h at 80 ˚C, the reaction mixture was diluted with chloroform and iso-propanol (4:1), neutralized with saturated $NaHCO_3$ and filtered. The filtrate was extracted with chloroform and iso-propanol (4:1), concentrated under reduced pressure and the resulting residue

was purified by silica gel column chromatography (MeOH/DCM = 0-20%) to give the compound **14**.

To a solution of **14** (0.034 mmol, 1 equiv) and DIEA (0.1 mmol, 3 equiv) in MeCN (2 mL) was added acryloyl chloride (0.044 mmol, 1.3 equiv) dropwise at 0 ^{o}C. When the reaction was completed, Na_2CO_3 aq.(sat.) was added, the resulting mixture was extracted with chloroform and iso-propanol (4:1) (20 mL x 2). The combined organic layer was concentrated and purified with Prep-HPLC (MeOH/H_2O, 0.05% TFA) to give compounds **1d-1f**.

*(R)-N-(4-(3-((5-(((5-(tert-butyl)oxazol-2-yl)methyl)thio)thiazol-2-yl)amino)piperidine-1-carbonyl)phenyl)acrylamide (**1d, MFH290**).* ^{1}H NMR (500 MHz, DMSO-d6) δ 10.27 (s, 1H), 7.98 (s, 1H), 7.85 – 7.57 (m, 2H), 7.49 – 7.27 (m, 2H), 7.15 – 6.81 (m, 1H), 6.71 (s, 1H), 6.44 (dd, J = 17.0, 10.2 Hz, 1H), 6.28 (dd, J = 17.0, 2.0 Hz, 1H), 5.78 (dd, J = 10.1, 2.0 Hz, 1H), 3.94 (s, 2H), 3.86 – 3.61 (m, 2H), 3.53 – 2.77 (m, 3H), 2.02 – 1.40 (m, 4H), 1.18 (s, 9H). MS (ESI) m/z 526.50 $[M + H]^+$;

*(S)-N-(4-(3-((5-(((5-(tert-butyl)oxazol-2-yl)methyl)thio)thiazol-2-yl)amino)piperidine-1-carbonyl)phenyl)acrylamide (**1e**).* ^{1}H NMR (500 MHz, DMSO-d_6) δ 10.31 (s, 1H), 8.08 (s, 1H), 7.80 – 7.60 (m, 2H), 7.46 – 7.28 (m, 2H), 7.00 – 6.82 (m, 1H), 6.71 (s, 1H), 6.43 (dd, *J* = 17.0, 10.1 Hz, 1H), 6.27 (dd, *J* = 17.0, 1.9 Hz, 1H), 5.78 (dd, *J* = 10.1, 1.9 Hz, 1H), 3.94 (s, 2H), 3.73 – 3.63 (m, 2H), 3.34 – 3.21 (m, 1H), 3.15 – 2.70 (m, 2H), 2.03 – 1.41 (m, 4H), 1.17 (s, 9H). MS (ESI) m/z 526.50 $[M + H]^+$;

*N-(4-((3-((5-(((5-(tert-butyl)oxazol-2-yl)methyl)thio)thiazol-2-yl)amino)cyclohexyl)amino)phenyl)acrylamide (**1f**).* ^{1}H NMR (500 MHz, DMSO-d6) δ 10.37 – 10.01 (m, 1H), 8.19 – 7.96 (m, 1H), 7.79 – 7.56 (m, 2H), 7.30 – 7.02 (m, 2H), 6.98

– 6.88 (m, 1H), 6.75 – 6.66 (m, 1H), 6.49 – 6.36 (m, 1H), 6.30 – 6.19 (m, 1H), 5.81 – 5.68 (m, 1H), 4.03 (s, 1H), 3.96 – 3.92 (m, 2H), 2.28 – 2.17 (m, 1H), 2.00 – 1.85 (m, 2H), 1.85 – 1.74 (m, 1H), 1.74 – 1.49 (m, 2H), 1.44 – 1.22 (m, 3H), 1.22 – 1.16 (m, 9H), 1.15 – 1.00 (m, 1H). MS (ESI) m/z 511.96 $[M + H]^+$;

Synthesis of compounds 1g-1i, 1k and 1l.

To a mixture of compound **11** (0.024 mmol, 1 equiv) in methanol (2 mL) was added 4N HCl/dioxane (2 mL). The resulted solution was stirred at rt for 3 h. The mixture was concentrated under reduced pressure to give the corresponding HCl salt. To a mixture of the HCl salt (0.024 mmol, 1 equiv), **12** (0.03 mmol, 1.3 equiv) and DIEA (0.12 mmol, 5 equiv) in DCM (2 mL) was added T_3P (50% solution in ethyl acetate, 46 mg, 0.07 mmol) dropwise at room temperature. The reaction mixture was stirred at room temperature overnight. The solution was diluted with DCM (20 mL) and washed with brine (50 mL × 2) and dried over Na_2SO_4, filtered and concentrated. The residue was purified by Prep-HPLC ($MeOH/H_2O$, 0.05% TFA) to give the compounds **1g-1i, 1k and 1l**.

*N-(4-((2R,3R)-3-((5-(((5-(tert-butyl)oxazol-2-yl)methyl)thio)thiazol-2-yl)amino)-2-methylpiperidine-1-carbonyl)phenyl)acrylamide (**1g**).* ^{1}H NMR (500 MHz, DMSO-d_6) δ 10.30 (s, 1H), 8.02 (s, 1H), 7.72 (d, *J* = 8.7 Hz, 2H), 7.38 (d, *J* = 8.2 Hz, 2H), 7.00 – 6.62 (m, 2H), 6.45 (dd, *J* = 17.0, 10.1 Hz, 1H), 6.28 (dd, *J* = 17.0, 2.0 Hz, 1H), 5.79 (dd, *J* = 10.1, 2.0 Hz, 1H), 3.94 (s, 2H), 3.86 – 3.70 (m, 2H), 3.14 – 2.57 (m, 2H), 1.81 – 1.44 (m, 4H), 1.17 (s, 9H), 1.04 (d, *J* = 6.9 Hz, 3H). MS (ESI) m/z 540.58 $[M + H]^+$;

*N-(4-(5-((5-(((5-(tert-butyl)oxazol-2-yl)methyl)thio)thiazol-2-yl)amino)-3,3-difluoropiperidine-1-carbonyl)phenyl)acrylamide (**1h**).* ^{1}H NMR (500 MHz, DMSO-d_6) δ 10.35 (s, 1H), 8.20 – 8.04 (m, 1H), 7.74 (d, *J* = 8.3 Hz, 2H), 7.42 (d, *J* = 8.5 Hz, 2H), 7.05

– 6.90 (m, 1H), 6.76 – 6.66 (m, 1H), 6.45 (dd, *J* = 17.0, 10.1 Hz, 1H), 6.29 (dd, *J* = 17.0, 2.0 Hz, 1H), 5.80 (dd, *J* = 10.1, 2.0 Hz, 1H), 3.96 (s, 2H), 3.78 – 3.50 (m, 4H), 2.16 – 2.06 (m, 1H), 1.90 – 1.65 (m, 2H), 1.22 (s, 9H). MS (ESI) m/z 562.54 $[M + H]^+$;

*N-(4-((2S,5R)-5-((5-(((5-(tert-butyl)oxazol-2-yl)methyl)thio)thiazol-2-yl)amino)-2-methylpiperidine-1-carbonyl)phenyl)acrylamide (**1i**).* ^{1}H NMR (500 MHz, DMSO-d_6) δ 10.30 (s, 1H), 8.03 (s, 1H), 7.73 (d, *J* = 8.7 Hz, 2H), 7.39 (d, *J* = 8.2 Hz, 2H), 6.93 (s, 1H), 6.71 (s, 1H), 6.45 (dd, *J* = 17.0, 10.1 Hz, 1H), 6.28 (dd, *J* = 17.0, 2.0 Hz, 1H), 5.79 (dd, *J* = 10.1, 2.0 Hz, 1H), 3.95 (s, 2H), 3.60 – 3.49 (m, 2H), 2.92 – 2.56 (m, 2H), 1.93 – 1.79 (m, 1H), 1.81 – 1.43 (m, 3H), 1.39 – 0.70 (m, 12H). MS (ESI) m/z 540.58 $[M + H]^+$;

*(R)-N-(4-(3-((5-(((5-(tert-butyl)oxazol-2-yl)methyl)thio)thiazol-2-yl)amino)piperidine-1-carbonyl)-2-fluorophenyl)acrylamide (**1k**).* ^{1}H NMR (500 MHz, DMSO-d_6) δ 10.06 (s, 1H), 8.21 – 7.87 (m, 2H), 7.31 (s, 1H), 7.22 – 7.16 (m, 1H), 6.80 (s, 1H), 6.75 – 6.69 (m, 1H), 6.66 (dd, *J* = 17.0, 10.2 Hz, 1H), 6.29 (dd, *J* = 16.9, 2.0 Hz, 1H), 5.80 (dd, *J* = 10.2, 2.0 Hz, 1H), 3.94 (s, 2H), 3.73 – 3.65 (m, 2H), 3.36 – 3.00 (m, 3H), 2.01 – 1.92 (m, 1H), 1.80 – 1.52 (m, 3H), 1.18 (s, 9H). MS (ESI) m/z 544.56 $[M + H]^+$;

*(R)-N-(4-(3-((5-(((5-(tert-butyl)oxazol-2-yl)methyl)thio)thiazol-2-yl)amino)piperidine-1-carbonyl)-2-(trifluoromethyl)phenyl)acrylamide (**1l**).* ^{1}H NMR (500 MHz, DMSO-d_6) δ 9.91 (s, 1H), 8.25 – 7.99 (m, 1H), 7.83 – 7.55 (m, 3H), 7.05 – 6.70 (m, 2H), 6.61 – 6.52 (m, 1H), 6.36 – 6.22 (m, 1H), 5.87 – 5.77 (m, 1H), 3.93 (s, 2H), 3.79 – 3.64 (m, 2H), 3.40 – 3.14 (m, 2H), 1.98 – 1.91 (m, 1H), 1.84 – 1.52 (m, 4H), 1.19 (s, 9H). MS (ESI) m/z 594.56 $[M + H]^+$;

Synthesis of compound 1s.

To a solution of (*R*)-(4-aminophenyl)(3-((5-(((5-(tert-butyl)oxazol-2-yl)methyl)thio)thiazol-2-yl)amino)piperidin-1-yl)methanone (**14**, 30 mg, 0.064 mmol) in DCM (2 mL) was added *m*-CPBA (12 mg, 0.07 mmol). The reaction mixture was stirred at room temperature overnight. Then diluted with DCM, washed with $NaHCO_3$ aq.(sat.), concentrated and purified with silica gel column (eluted with MeOH in DCM 0% to 15%) to give the sulfoxide intermediate (20 mg, 64%) as a brown oil. To the solution of resulting sulfoxide (20 mg, 0.04 mmol) in MeCN (2 mL) was added DIEA (25 mg, 0.2 mmol). At 0 ^oC acryloyl chloride (4 mg, 0.044 mmol) was added dropwise. When the reaction was completed, Na_2CO_3 aq.(sat.) was added. The resulting mixture was extracted with chloroform and iso-propanol (4:1) (20 mL x 2). The combined organic layer was concentrated and purified with Prep-HPLC (MeOH/H_2O, 0.05%TFA) to give compound **1s** (8 mg, 36.9%) as white solid.

*N-(4-((3R)-3-((5-(((5-(tert-butyl)oxazol-2-yl)methyl)sulfinyl)thiazol-2-yl)amino)piperidine-1-carbonyl)phenyl)acrylamide **(1s)**.* ^1H NMR (500 MHz, DMSO-d_6) δ 10.18 (s, 1H), 8.45 (s, 1H), 7.59 (s, 2H), 7.47 – 7.00 (m, 3H), 6.68 (s, 1H), 6.43 – 6.27 (m, 1H), 6.25 – 6.08 (m, 1H), 5.76 – 5.58 (m, 1H), 4.53 – 4.32 (m, 2H), 3.97 – 3.38 (m, 3H), 3.34 – 2.81 (m, 2H), 1.98 – 1.80 (m, 1H), 1.77 – 1.31 (m, 3H), 1.04 (s, 9H). MS (ESI) m/z 542.55 $[M + H]^+$;

Synthesis of compounds 1m-o, 1u, 1v.

A mixture of **15** (3 mmol, 1 equiv) and potassium thiocyanate (30 mmol, 10 equiv) in methanol (20 mL) was stirred at room temperature for 48 hours. Methanol was evaporated and water (3 ml) was added. The pH of the aqueous solution was adjusted to

pH=12 with 10% NaOH aq and precipitate formed. The solid was collected by filtration to yield compounds **16**.

To a solution of compound **16** (1 mmol, 1 equiv) in absolute ethanol (3 ml) was added $NaBH_4$ (2 mmol, 2 equiv) portionwise at 0 ^oC. The mixture was stirred at room temperature for 1 h, and then acetone (2 ml) was slowly introduced. After 1 hour, a solution of appropriate halide (1.1 mmol, 1.1 equiv) in ethanol (2 ml) was added. The resulting dark reaction mixture was heated to 65 ^oC for 1 hour and was then cooled and concentrated in vacuo. The residue was partitioned between ethyl acetate and brine. The organic phase was separated, dried over $MgSO_4$, concentrated and purified with silica gel column (MeOH/DCM, 0-10%) to provide the compound **17**.

To a solution of $CuBr_2$ (1.9 mmol, 1.7 equiv) in acetonitrile (10 mL) at 0°C was added t-BuONO (1.9 mmol, 1.7 equiv) followed by compound **17** (1.1 mmol, 1 equiv). The mixture was stirred at 0 °C for 1 hour, then at room temperature for 1 hour. Ethyl acetate was added, and the organic layer was washed with 1N hydrochloric acid (2 x 50 mL), dried over magnesium sulfate, filtered through a pad of silica gel, and concentrated in vacuo. The residue was purified on silica gel column (ethyl acetate in hexane, 0-50%) to give the compound **18**.

A mixture of **18** (0.4 mmol, 1 equiv.), tert-butyl (*R*)-3-aminopiperidine -1-carboxylate (0.8 mmol, 2 equiv), DIEA (1.2 mmol, 3 equiv) in NMP (3 mL) was heated to 140 °C overnight. The solution was diluted with water (20 mL) and extracted with chloroform and iso-propanol (4:1). The organic phase was washed with brine (50 mL × 2) and dried over Na_2SO_4, filtered and concentrated. The residue was purified by silica gel column (MeOH/DCM, 0-20%) to give compound **19**.

To a mixture of compound **19** (0.47 mmol, 1 equiv) in methanol (2 mL) was added 4N HCl/dioxane (2 mL) and the resulted solution was stirred at room temperature for 3 h. The mixture was concentrated, and the residue was purified by Prep-HPLC (MeOH/H_2O, 0.05% TFA) to give the compound **20**.

To a mixture of **20** (22 mg, 0.06 mmol), 4-acrylamidobenzoic acid (14 mg, 0.072 mmol) and DIEA (39 mg, 0.3 mmol) in DCM (2 mL) was added T_3P (50% solution in ethyl acetate, 57 mg, 0.18 mmol) dropwise at RT. The reaction mixture was stirred at RT overnight. The solution was diluted with DCM (20 mL) and washed with brine (50 mL × 2) and dried over Na_2SO_4, filtered and concentrated. The residue was purified by Prep-HPLC (MeOH/H_2O, 0.05% TFA) to give the compound **1m-o, 1u** and **1v**.

*(R)-N-(4-(3-((5-((pyridin-4-ylmethyl)thio)thiazol-2-yl)amino)piperidine-1-carbonyl)phenyl)acrylamide (**1m**).* ^{1}H NMR (500 MHz, DMSO-d_6) δ 10.30 (s, 1H), 8.41 – 7.57 (m, 5H), 7.36 (s, 2H), 7.25 – 7.02 (m, 2H), 6.81 (s, 1H), 6.43 (dd, *J* = 17.4, 9.7 Hz, 1H), 6.27 (d, *J* = 17.0 Hz, 1H), 5.78 (d, *J* = 10.3 Hz, 1H), 3.99 (s, 2H), 3.44 – 2.75 (m, 5H), 2.02 – 1.66 (m, 2H), 1.66 – 1.37 (m, 2H). MS (ESI) m/z 479.96 $[M + H]^+$;

*(R)-N-(4-(3-((5-(((2-(trifluoromethyl)pyrimidin-5-yl)methyl)thio)thiazol-2-yl)amino)piperidine-1-carbonyl)phenyl)acrylamide (**1n**).* ^{1}H NMR (500 MHz, DMSO-d6) δ 10.26 (s, 1H), 8.81 (s, 2H), 8.10 (s, 1H), 7.92 – 7.59 (m, 2H), 7.51 – 7.23 (m, 2H), 7.12 – 6.72 (m, 1H), 6.56 – 6.35 (m, 1H), 6.35 – 6.16 (m, 1H), 5.87 – 5.68 (m, 1H), 4.01 (s, 2H), 3.42 – 2.82 (m, 5H), 2.02 – 1.87 (m, 1H), 1.85 – 1.63 (m, 1H), 1.63 – 1.39 (m, 2H). MS (ESI) m/z 548.89 $[M + H]^+$;

*(R)-N-(4-(3-((5-(((tetrahydro-2H-pyran-4-yl)methyl)thio)thiazol-2-yl)amino)piperidine-1-carbonyl)phenyl)acrylamide (**1o**).* ^{1}H NMR (500 MHz, DMSO-d_6) δ 10.29 (s, 1H), 8.07 (s,

1H), 7.86 – 7.57 (m, 2H), 7.52 – 7.31 (m, 2H), 7.19 – 6.88 (m, 1H), 6.45 (dd, *J* = 17.0, 10.1 Hz, 1H), 6.28 (dd, *J* = 16.9, 2.0 Hz, 1H), 5.79 (dd, *J* = 10.1, 2.0 Hz, 1H), 3.90 – 3.78 (m, 2H), 3.24 (t, *J* = 11.5 Hz, 2H), 3.15 – 2.95 (m, 1H), 2.64 – 2.54 (m, 2H), 2.03 – 1.46 (m, 6H), 1.40 – 1.03 (m, 3H). MS (ESI) m/z 487.31 $[M + H]^+$;

*(R)-N-(4-(3-((5-(((5-(tert-butyl)oxazol-2-yl)methyl)thio)-1,3,4-thiadiazol-2-yl)amino)piperidine-1-carbonyl)phenyl)acrylamide (**1u**).* ^{1}H NMR (500 MHz, DMSO-d_6) δ 10.29 (s, 1H), 8.02 (d, J = 6.9 Hz, 1H), 7.68 (s, 2H), 7.36 (s, 2H), 6.75 (s, 1H), 6.44 (dd, J = 16.9, 10.1 Hz, 1H), 6.27 (dd, J = 17.0, 2.0 Hz, 1H), 5.78 (dd, J = 10.0, 2.0 Hz, 1H), 4.33 (s, 2H), 4.01 – 3.63 (m, 3H), 3.35 – 2.96 (m, 2H), 2.07 – 1.42 (m, 4H), 1.18 (s, 9H). MS (ESI) m/z 526.98 $[M + H]^+$;

*(R)-N-(4-(3-((5-(((5-(tert-butyl)oxazol-2-yl)methyl)thio)-4-methylthiazol-2-yl)amino)piperidine-1-carbonyl)phenyl)acrylamide (**1v**).* ^{1}H NMR (500 MHz, DMSO-d_6) δ 10.28 (s, 1H), 8.05 (s, 1H), 7.76 – 7.58 (m, 2H), 7.35 (s, 2H), 6.70 (s, 1H), 6.44 (dd, J = 17.0, 10.2 Hz, 1H), 6.28 (dd, J = 17.0, 2.0 Hz, 1H), 5.78 (dd, J = 10.1, 2.0 Hz, 1H), 3.87 (s, 2H), 3.70 – 3.55 (m, 2H), 3.28 – 3.01 (m, 3H), 1.96 – 1.84 (m, 2H), 1.62 – 1.44 (m, 5H), 1.17 (s, 9H). MS (ESI) m/z 540.54 $[M + H]^+$;

Synthesis of compound 1j.

To the mixture of **20** (0.12 mmol, 1 equiv), 5-nitropicolinic acid (0.14 mmol, 1.2 equiv) and DIEA (0.6 mmol, 5 equiv) in DCM (2 mL) was added T_3P (50% solution in ethyl acetate, 0.36 mmol, 3 equiv) dropwise at room temperature. The reaction mixture was stirred at room temperature overnight. The solution was diluted with DCM (20 mL) and washed with brine (50 mL × 2) and dried over Na_2SO_4, filtered and concentrated. The residue was purified by silica gel column (MeOH/DCM, 0-20%).

To the solution of the resulting intermediate (0.54 mmol, 1 equiv) in ethyl acetate and methanol (1:1) were added Tin(II) chloride dehydrate (5.4 mmol, 10 equiv) and conc. HCl (0.2 mL). After stirring for 3 h at 80 ˚C, the reaction mixture was diluted with chloroform and iso-propanol (4:1), neutralized with saturated $NaHCO_3$ and filtered. The filtrate was extracted with chloroform and iso-propanol (4:1), concentrated under reduced pressure and the resulting residue was purified by silica gel column chromatography (MeOH/DCM = 0-20%) to give the corresponding amine intermediate.

To a solution of amine intermediate (0.05 mmol, 1 equiv) in THF (5 mL) was added DIEA (0.15 mmol, 3 equiv) and acryloyl chloride (0.05 mmol, 1 equiv) at 0 ºC for 30 min. The resulting mixture was stirred at room temperature for 2 hours. The solution was concentrated and purified by silica gel column (MeOH/DCM, 0-20%) to afford the compound **1j** as a slightly white solid.

*(R)-N-(6-(3-((5-(((5-(tert-butyl)oxazol-2-yl)methyl)thio)thiazol-2-yl)amino)piperidine-1-carbonyl)pyridin-3-yl)acrylamide (**1j**).* ^{1}H NMR (500 MHz, Methanol-d4) δ 8.93 – 8.51 (m, 1H), 8.29 – 7.89 (m, 1H), 7.49 (s, 1H), 7.19 – 6.79 (m, 1H), 6.74 – 6.53 (m, 1H), 6.42 – 6.15 (m, 2H), 5.87 – 5.68 (m, 1H), 4.24 – 3.81 (m, 3H), 3.80 – 3.23 (m, 4H), 2.14 – 1.47 (m, 4H), 1.15 (s, 9H). MS (ESI) m/z 527.52 $[M + H]^+$;

Synthesis of compound 1t.

A mixture of 2,4,5-trichloropyrimidine (**21**) (500 mg, 2.7 mmol) and potassium thiocyanate (1.1 g, 10.9 mmol) in methanol (10 mL) was stirred at room temperature for 48 hours. Methanol was evaporated and water (3 ml) was added. The pH of the aqueous solution was adjusted to pH=12 with 10% NaOH aq. and precipitate formed. The solid was collected by filtration to yield compound **22**.

To a solution of compound **22** (300 mg, 1.5 mmol) in absolute ethanol (3 ml) was added $NaBH_4$ (110 mg, 2.9 mmol) portionwise at 0 ^oC. The mixture was stirred at room temperature for 1 hour, and then acetone (3 ml) was slowly introduced. After 1 hour, a solution of 5-(tert-butyl)-2-(chloromethyl)oxazole (253 mg, 1.46 mmol) in ethanol (5 ml) was added. The resulting dark reaction mixture was heated to 65 ^oC for 1 hour and was then cooled and concentrated in vacuo. The residue was partitioned between ethyl acetate and brine. The organic phase was separated, dried over $MgSO_4$, concentrated and purified with silica gel column (eluted with MeOH in DCM 0% to 10%) to provide the compound **23**.

A mixture of **23** (78 mg, 0.25 mmol), tert-butyl (*R*)-3-aminopiperidine -1-carboxylate (74 mg, 0.37 mmol), DIEA (63 mg, 0.49 mmol) in NMP (1 mL) was heated to 140 °C overnight. The solution was diluted with water (20 mL) and extracted with chloroform and iso-propanol (4:1). The organic phase was washed with brine (50 mL × 2) and dried over Na_2SO_4, filtered and concentrated. The residue was purified by silica gel column (MeOH/DCM, 0-20%) to give compound **24**.

To a mixture of **24** (120 mg, 0.25 mmol) in methanol (4 mL) was added 4N HCl/dioxane (4 mL). The resulted solution was stirred at room temperature for 3 hours. The mixture was concentrated under reduced pressure to give the corresponding HCl salt. To the solution of HCl salt (95 mg, 0.25 mmol) in pyridine (2 mL) was added 4-nitrobenzoyl chloride (56 mg, 0.3 mmol), the reaction mixture was stirred at room temperature overnight. The resulting mixture was concentrated under reduced pressure and the residue was purified by silica gel column (MeOH/DCM, 0-20%) to give compound **25**.

To a solution of **25** (133 mg, 0.25 mmol) in ethyl acetate and methanol (1:1, 3 ml/ 3 ml) were added Tin(II) chloride dehydrate (339 mg, 1.5 mmol) and conc. HCl (0.2 mL). After stirring for 3 hours at 80 ˚C, the reaction mixture was diluted with chloroform and iso-propanol (4:1), neutralized with saturated $NaHCO_3$ and filtered. The filtrate was extracted with chloroform and iso-propanol (4:1), concentrated under reduced pressure and the resulting residue was purified by silica gel column chromatography (MeOH/DCM = 0-20%) to give the compound **26**.

To a solution of compound **26** (25 mg, 0.05 mmol) and DIEA (19 mg, 0.15 mmol) in MeCN (2 mL) was added acryloyl chloride (5 mg, 0.06 mmol) dropwise at 0 ^oC. When the reaction was completed, Na_2CO_3 aq.(sat.) was added, the resulting mixture was extracted with chloroform and iso-propanol (4:1) (20 mL x 2). The combined organic layer was concentrated and purified with Prep-HPLC (MeOH/H_2O, 0.05% TFA) to give compound **1t**.

*(R)-N-(4-(3-((4-(((5-(tert-butyl)oxazol-2-yl)methyl)thio)-5-chloropyrimidin-2-yl)amino)piperidine-1-carbonyl)phenyl)acrylamide (**1t**).* ^1H NMR (500 MHz, DMSO-d_6) δ 10.26 (s, 1H), 8.09 (s, 1H), 7.86 – 6.99 (m, 5H), 6.72 (s, 1H), 6.44 (dd, J = 16.9, 10.2 Hz, 1H), 6.28 (dd, J = 17.0, 2.0 Hz, 1H), 5.78 (dd, J = 10.1, 2.0 Hz, 1H), 4.86 – 4.32 (m, 2H), 3.95 – 3.64 (m, 2H), 3.17 (s, 2H), 2.94 – 2.63 (m, 1H), 2.02 – 1.71 (m, 2H), 1.66 – 1.39 (m, 2H), 1.20 (s, 9H). MS (ESI) m/z 554.93 $[M + H]^+$;

Synthesis of compound 1p.

A solution of 5-(tert-butyl)-2-(chloromethyl)oxazole (**27**) (800 mg, 4.61 mmol) in triethyl phosphite (3.83 g, 23.04 mmol) was heated at 120 °C overnight. The solvent was

removed under reduced pressure to provide a crude **28** which was directly used in the next step.

To a solution of **28** (500 mg, 1.82 mmol) in THF (5 mL) was added t-BuOK (370 mg, 3.3 mmol) portionwise at room temperature. The vial was sealed and stirred at room temperature for 10 mins. Then, a solution of tert-butyl 5-formylthiazol-2-ylcarbamate (345 mg, 1.5 mmol) in THF (3 mL) was added in the reaction mixture. After completion, the reaction mixture was quenched with water. The obtained mixture was extracted with chloroform and iso-propanol (4:1). The organic phase was washed with brine (50 mL × 2) and dried over Na_2SO_4. After removal of the solvent, the residue was purified by silica gel (MeOH/DCM = 0-20%) to obtain compound **30.**

A mixture of compound **30** (250 mg, 1 mmol) and 10% Pd/C (20 mg) in MeOH (10 mL) was stirred for 5 hours at room temperature under H_2 balloon. The mixture was filtered through Celite. The filtrate was added 4N HCl/dioxane (5 mL). The solution was then stirred for 3 hours at room temperature and the solvent was removed under reduced pressure to provide compound **31** as HCl salt which was directly used in the next step.

To a solution of $CuBr_2$ (53 mg, 0.24 mmol) in acetonitrile (2 mL) at 0°C was added t-BuONO (25 mg, 0.24 mmol) followed by compound **31** (60 mg, 0.24 mmol). The mixture was stirred at 0°C for 1 hour, then at room temperature for 1 hour. Ethyl acetate was added, and the organic mixture was washed with 1N hydrochloric acid (2 x 20 mL), dried over magnesium sulfate, filtered through a pad of silica gel, and concentrated in vacuo. The residue was chromatographed on silica gel (ethyl acetate in hexane, 0-50%) to give the compound **32**.

The mixture of **32** (40 mg, 0.13 mmol), (*R*)-tert-butyl 3-aminopiperidine-1-carboxylate (41 mg, 0.2 mmol) and DIEA (33 mg, 0.25 mmol) in NMP (0.5 mL) was stirred at 140 °C for overnight. The residue was extracted with chloroform and iso-propanol (4:1). The organic phase was washed with brine (10 mL × 2) and dried over Na_2SO_4. After removal of the solvent, the residue was purified by silica gel (MeOH/DCM = 0-20%) to obtain the compound **33.**

To a solution of compound **33** (35 mg, 0.08 mmol) in methanol (2 mL) was added 4N HCl/dioxane (2 mL). The solution was then stirred for 3 hours at room temperature and the solvent was removed under reduced pressure to provide **34** as HCl salt which was directly used in the next step.

The mixture of compound **34** (23 mg, 0.07 mmol), 4-acrylamidobenzoic acid (15 mg, 0.08 mmol), HOBT (12 mg, 0.09 mmol) and EDCI (17 mg, 0.09 mmol) in DMF (0.5 ml) was stirred at room temperature overnight. The reaction mixture was purified by prep-HPLC ($MeOH/H_2O$, 0.05%TFA) to provide compound **1p**.

*(R)-N-(4-(3-((5-(2-(5-(tert-butyl)oxazol-2-yl)ethyl)thiazol-2-yl)amino)piperidine-1-carbonyl)phenyl)acrylamide (**1p**).* ^{1}H NMR (500 MHz, DMSO-d_6) δ 10.39 (s, 1H), 8.30 (d, *J* = 7.5 Hz, 1H), 7.83 (d, *J* = 8.8 Hz, 2H), 7.75 (d, *J* = 8.8 Hz, 2H), 6.96 (s, 1H), 6.69 (s, 1H), 6.46 (dd, *J* = 17.0, 10.1 Hz, 1H), 6.29 (dd, *J* = 17.0, 1.9 Hz, 1H), 5.80 (dd, *J* = 10.1, 1.9 Hz, 1H), 4.03 – 3.83 (m, 2H), 3.68 (d, *J* = 12.8 Hz, 1H), 3.14 – 2.91 (m, 6H), 2.01 – 1.79 (m, 2H), 1.68 – 1.54 (m, 2H), 1.22 (s, 9H). MS (ESI) m/z 508.07 $[M + H]^+$;

Synthesis of compound 1q and 1r.

The mixture of (2-bromothiazol-5-yl)methanol (**35**) (220 mg, 1.1 mmol), 5-tert-butyl-2-(chloromethyl)oxazole (**27**) (256 mg, 1.5 mmol) and NaOH (82 mg, 2.04mmol) in DMF (2

mL) was stirred at 120 °C for 3 hours. The residue was extracted with chloroform and iso-propanol (4:1). The organic phase was washed with brine (20 mL × 2) and dried over Na_2SO_4. After removal of the solvent, the residue was purified by silica gel (PE/EA = 0-50%) to obtain compound **36**.

The mixture of **36** (170 mg, 0.51 mmol), (*R*)-tert-butyl 3-aminopiperidine-1-carboxylate (164 mg, 0.82 mmol) and DIEA (133 mg, 1 mmol) in NMP (1 mL) was stirred at 140 °C for overnight. The residue was extracted with chloroform and iso-propanol (4:1). The organic phase was washed with brine (20 mL × 2) and dried over Na_2SO_4. After removal of the solvent, the residue was purified by silica gel (MeOH/DCM = 0-20%) to obtain compound **41a**.

The mixture of compound **38** (800 mg, 4.23 mmol), (*R*)-tert-butyl 3-aminopiperidine-1-carboxylate (1.1 g, 5.5 mmol) and DIEA (820 mg, 6.35 mmol) in THF (15 mL) was stirred at 80 °C for 6 hours. The residue was extracted with chloroform and iso-propanol (4:1). The organic phase was washed with brine (50 mL × 2) and dried over Na_2SO_4. After removal of the solvent, the residue was purified by silica gel (MeOH/DCM = 0-20%) to obtain compound **39**.

To a solution of **39** (300 mg, 1 mmol) and $CoCl_2$-$6H_2O$ (232 mg, 1 mmol) in ethanol (8 mL) was added $NaBH_4$ (110 mg, 3 mmol) portionwise at room temperature. The vial was sealed and stirred at room temperature for 3 hours. And then quenched with water. The obtained mixture was extracted with chloroform and iso-propanol (4:1). The organic phase was washed with brine (50 mL × 2) and dried over Na_2SO_4. After removal of the solvent, the residue was purified by silica gel (MeOH/DCM = 0-20%) to obtain compound **40**.

The mixture of compound **40** (160 mg, 0.51 mmol), 5-tert-butyl-2-(chloromethyl)oxazole (**27**) (89 mg, 0.51 mmol) and DIEA (132 mg, 1 mmol) in NMP (1 mL) was stirred at 80 °C overnight. The residue was extracted with chloroform and iso-propanol (4:1). The organic phase was washed with brine (50 mL × 2) and dried over Na_2SO_4. After removal of the solvent, the residue was purified by silica gel (MeOH/DCM = 0-20%) to obtain compound **41b**.

The mixture of compound **41** (0.07 mmol, 1 equiv.), 4-acrylamidobenzoic acid (0.08 mmol, 1.1 equiv), HOBT (0.09 mmol, 1.3 equiv) and EDCI (0.09 mmol, 1.3 equiv) in DMF (0.5 ml) was stirred at room temperature overnight. The reaction mixture was purified by prep-HPLC (MeOH/H_2O, 0.05%TFA) to provide compound **1q** and **1r**.

*(R)-N-(4-(3-((5-(((5-(tert-butyl)oxazol-2-yl)methoxy)methyl)thiazol-2-yl)amino)piperidine-1-carbonyl)phenyl)acrylamide (**1q**).* ^{1}H NMR (500 MHz, DMSO-d_6) δ 10.38 (s, 1H), 8.51 – 8.23 (m, 1H), 7.84 (d, J = 8.5 Hz, 2H), 7.75 (d, J = 8.4 Hz, 2H), 7.49 – 6.91 (m, 1H), 6.74 (s, 1H), 6.46 (dd, *J* = 17.0, 10.1 Hz, 1H), 6.29 (dd, *J* = 16.9, 2.1 Hz, 1H), 5.80 (d, *J* = 10.0 Hz, 1H), 4.43 (s, 2H), 4.17 – 3.84 (m, 3H), 3.17 (s, 2H), 3.11 – 2.73 (m, 2H), 2.17 – 1.42 (m, 4H), 1.25 (s, 9H). MS (ESI) m/z 524.03 $[M + H]^+$;

*(R)-N-(4-(3-((5-((((5-(tert-butyl)oxazol-2-yl)methyl)amino)methyl)thiazol-2-yl)amino)piperidine-1-carbonyl)phenyl)acrylamide (**1r**).* ^{1}H NMR (500 MHz, DMSO-d_6) δ 10.31 (s, 1H), 8.83 – 8.60 (m, 2H), 8.09 – 7.63 (m, 3H), 7.37 (s, 1H), 6.96 (d, *J* = 10.8 Hz, 1H), 6.78 (d, *J* = 1.4 Hz, 1H), 6.57 – 6.36 (m, 1H), 6.35 – 6.19 (m, 1H), 5.86 – 5.71 (m, 1H), 4.38 – 4.27 (m, 4H), 3.79 – 3.68 (m, 3H), 2.95 – 2.77 (m, 2H), 2.03 – 1.85 (m, 2H), 1.69 – 1.51 (m, 2H), 1.26 (s, 9H). MS (ESI) m/z 523.21 $[M + H]^+$;

Cell culture

In this study, Jurkat cell lines (A.T. Look Laboratory, DFCI) were grown in RPMI 1640, Glutamax (Life Technologies) supplemented with 10% FBS (Life Technologies). HAP1 cells (Horizon Discovery Group, cat # C859) were grown in IMDM medium supplemented (Life Technologies) with 10% FBS and 100 U/ml penicillin, 100 mg/ml (Life Technologies). All cell lines were cultured at 37 °C in a humidified chamber in the presence of 5% CO2, unless otherwise noted. All cells were mycoplasma tested upon initial receipt.

Constructs

For CRISPR studies, guide RNAs (sgRNA) targeting CDK12 and CDK13 were cloned into pX330 (Addgene: 42230). pUC57-AMP was used as storage vector for CDK12 and CDK13 genome reference sequence.

Genome Editing

The CRISPR/Cas9 system was used to mutate the endogenous CDK12 and CDK13 WT loci to encode for CDK12 C1039S and CDK13 C1017S, respectively. Target-specific oligonucleotides were cloned into pX330 (Addgene: 42230), which carries a codon-optimized version of Cas9 and was further modified to express GFP for identifying transfectants. Cells were co-transfected (X-tremeGENE 9 (Roche)) with 1) pX330 expressing Cas9 and CDK12 (or CDK13) targeting sgRNA, and 2) a pUC57-AMP construct bearing 1500 bp of modified CDK12 (or CDK13) reference genome that is centered around the CRISPR targeting site in CDK12 (or CDK13). Two days after transfection, cells were sorted using GFP as a marker of transfected cells and cells were

re-plated for five days. Cells were then re-plated at low density to facilitate the isolation of individual clones. Individual clones were isolated, expanded, and PCR genotyped using mutant specific PCR primers. Following initial PCR screening, individual clones were Sanger sequenced to confirm the presence of the desired mutation. To generate a CDK12 C1039S/ CDK13 C1017S double mutant clone, mutations were serially performed, sequenced verified, and re-subjected to further mutagenesis. Western blot confirmed the presence of intact CDK12 (or CDK13) kinase. Subsequent experiments were conducted using a CDK12 C1039S clone, a CDK13 C1017S clone, a CDK12 C1039S/ CDK13 C1017S double mutant clone, and a WT control clone that was carried through the entirety of the CRISPR protocol but that was verified by Sanger sequencing to be WT CDK12 and CDK13.

For CDK12:

Guide RNA and repair template composition was previously described[5].

For CDK13:

The genomic sequence complementary to the CDK13 -directed guide RNA that was cloned into pX330 and used in the genome editing experiments is: GGCAAGATTGTCATGAGTTA.

The modified genomic sequence that was cloned into pUC57-AMP by Genewiz and used as the repair template for genome editing is:

GCCATGAGGAGTCGACGGATTATAGGCGTGAGCCACTGTGCCTGGCTGGAAATG
GCATATTTTTCTGCCTTCTTTTTCATGTCTTATTCAGTGTATGATGTACTATCATAAG
AACTGACTTTGAAAGGTTGCACCAACAGCAATAGTGGTGTTTTTTTTTTTTTTTTTT

TGAGACGGAGTCTCGCTGTGTCACCCAGGCTGGAGTGCAGTGGCGCAATCTCGG

CTCACCGCAACCTCCACCTCCCGGGTTCATGCCATTCTCCTGCCTCAGCCTCCTGA

GTAGCTGGGATTACAGGTGCCCGCCACCACGCCTGGCTAATTTTTGTATTTTTAGT

AGAAACGGGGTTTTGCCATGTTGGCCAGGCTGATCTCAAACTCCTGACCTCAGAT

GATCCACCTATGTCGGCCTCCCAAAGTGCTGGGATTACAGGCATGCCCAGCATAG

TAGCCTATTTTTATGAATATATATTCTTCATTCATAATTTTGATAAATGATTATTTATT

GATTATTCAAAAGCCAAAGAAAAATAGATTATCTGTAAAGGCAAAGCAAGCCCTGA

AGGAAGTGGGACAATAAGGATGATTTTTATTGGAAGAGTTTTACAGAGCCATTCTAT

GAAGTCTTCAAGAACTATTTGGGGTGGGGGCATAACTTTGTTGCTATATAGTAACT

GTAGCATTTTTTGTTAAGAAATGCCATTTACAATTTAATTCCTTTTTTTTTTTTCAGTCT

CCCTTTATGGCAGGACTCTCACGAGCTCTGGAGTAAAAAGCGAAGAAGACAGAAG

CAGATGGGCATGACTGATGATGTTTCCACAATTAAAGCCCCCAGGAAGGACTTGTC

TCTGGGCTTGGATGACAGCAGAACCAACACACCCCAGGGTGTGCTGCCATCTTCA

CAGCTGAAATCTCAGGGCAGCTCAAATGTGGCACCTGGTCAGTAATGCTTCCATG

GGTTGGTTTTCTTCACATTGTTTTGCAGTTAATTCTGATCATATTGCTCTAATGTTAA

AGCATCTTGTGGCTAACAATGAAAATTAACATTTATTCACTGAACTAGACATTTCTTT

GTGCCAGTACAGAAGTTTCATTGCTATTGGCACCACAATTTTAAGTAATCTTAAGGT

AACTTATAAAGAAGCATCAAATTACCTGACTGGCAAGTCCTCGGATTTCTGTATTTC

CTTTTTACTCTTAGTGCAGGAGTGAGTAGGTCTTTTACTGACACTACTCTCAGTGAG

GCTCAGCATTCAATGTCTATAGATGCTTAAGCAGTAGGAAGAAAGGTATAAGAAAA

CAGCCAAAAATCATAATGAGAGCTCTTTCATACCATTTATAGCGTCCTCATGTCACT

CCTAATGTTATAATTTCTCTGGTTATATTAAAGAATCTTAAAGATTGGGGCCAGGCA

TGCTGGCTCACGCCTGTAATCCTAGCACTTTGGGAGACTGAGGCGGATGGATCAC

CTGAGATCAGGAGTTCGAGAATTCTCGAGTACCG

1. Green highlighting indicates the introduced desired TCT mutation, which codes for serine (C1017S), replacing TGT which codes for cysteine (C1039, WT)
2. Yellow highlighting indicates wobble mutations introduced to (1) remove Cas9 – targeting PAM sites, to prevent cutting of repair template and (2) enable PCR-based screening to permit WT vs. mutated allele discrimination.
3. Red highlighting indicates Sal I and EcoRI sites used for pUC57 cloning.

Reagents and Antibodies

The following antibodies were used for immunoblots: Pol II CTD Ser-2 (cat# 04 1571), Ser-5 (cat# 04-1572), and Ser-7 (cat# 04-1570) phospho-antibodies (Millipore); Total Pol II (Santa Cruz cat# sc-899); CDK12 (Cell Signaling cat# 11973); cyclin K (Bethyl cat# A301-939A); cyclin H (Bethyl cat# A301-674A); RAD51 (Santa Cruz cat# sc-8349); RAD51C (Novus Biologicals cat# NB100-177); and BRCA2 (Millipore cat# OP95)and α-Tubulin DM1α (Sigma cat# T9026).

Immunoblotting

Whole cell lysates for immunoblotting were prepared by pelleting cells from each cell line at 4^{o}C (1,200 rpm) for 5 min using a Sorvall Legend centrifuge (Thermo Fisher Scientific). The resulting cell pellets were washed 1X with ice-cold 1X PBS and then resuspended in lysis buffer containing 50 mM TrisHCl pH 8.0, 150 mM NaCl, 1% NP-40, 0.1% SDS, 5

mM EDTA with protease (Roche cat# 04 693 159 001) and phosphatase inhibitors (Roche cat# 04 906 837 001). Whole cell lysates were collected and snap-frozen in liquid nitrogen before being stored at -80ºC. Protein concentrations were determined by using the Biorad DC protein assay kit (Bio-Rad, #500-0111) or Pierce BCA protein assay kit (Life Technologies #23225). Whole cell lysates were loaded into Bolt 4-12% or 8% bis-tris gels (Invitrogen, Carlsbad,CA) and separated by electrophoresis at 90 V for 2 hr. The gels were then transferred onto nitrocellulose membrane (Biorad cat# 162-0115) and blocked by incubation with 5% dry milk or BSA in TBST (TBS with 0.2% Tween-20). Membranes were probed using antibodies raised against the indicated proteins. Appropriate IR-labeled secondary antibodies were used and Licor Odyssey CLx was used for detection.

Pull down/Immunoprecipitation (IP) experiments.

Cells were treated with MFH290 or DMSO for 6 hrs. Following treatment cells were washed 2-fold with cold PBS and then lysed in the following lysis buffer: 50 mM Hepes pH 7.4, 150 mM NaCl, 1% Nonidet P40 substitute, 5 mM EDTA, 1mM DTT, and protease/phosphatase cocktails. Following clearance, lysates were treated with bio-THZ1 for pulldown overnight at 4 ºC. Lysates were further incubated at room temperature for 3 hrs to increase the efficiency of covalent bond formation. Lysates were then incubated with streptavidin agarose (Thermo scientific cat. #20349)) for pulldown for an additional 2-3 hrs at 4ºC. Agarose beads were washed 6 times with lysis buffer and then boiled in 2X SDS page loading buffer for 10 minutes at 95 ºC. SDS-page resolved precipitated proteins were probed for the indicated proteins.

Enzymatic Assays.

The enzymatic activities against CDK1, 2 and 5 were tested in Z'-Lyte assays with ATP concentrations of Km. The activities against CDK3, 8, 14 and 16 were tested in LanthaScreen™ Eu Kinase Binding assays. The activities against CDK4, 6, 7 and 9 were tested in Adapta assays. The activity against CDK12 and 13 was tested in radioisotope filter binding assay. All the protocols are available from Life Technologies and Reaction Biology.

Kinome Profiling.

Kinome profiling was performed using KinomeScan ScanMAX at compound concentration of 1 μM. Data was reported in Supplementary data. Protocols are available from DiscoverX.

Proliferation Assays

Proliferation assays were conducted using CellTiter Glo ® assay kit (Promega cat# G7571). For 72-hr studies, HAP1 cells were plated in 96-well plates at 25,000 cells/well in fresh media. Twenty-four hours later, cells were treated with MFH290 at the indicated concentrations or DMSO for 72 hours. For 8-day synergy studies, HAP1 cells were seeded in 96-well plates at 5,000 cells/well in fresh media. Twenty-four hours later cells were treated with MFH290 +/- olaparib at the indicated concentrations 8 days. Anti-proliferative effects of compounds were assessed using CellTiter Glo ® as described in product manual by luminescence measurements on an Envision plate reader.

Mass spectrometry analysis

CDK12/Cyclin K complex (5 µg) was treated with DMSO or a 10-fold molar excess of MFH-2-90 for 1 hour at room temperature and analyzed by LC-MS using an HPLC system (Shimadzu, Marlborough, MA) interfaced to an LTQ ion trap mass spectrometer (ThermoFisher Scientific, San Jose, CA). After injection, proteins were desalted for 4 minutes on column with 100% A, and then eluted with an HPLC gradient (0-100% B in 1 minute; A=0.2M acetic acid in water; B=0.2M acetic acid in acetonitrile). The mass spectrometer was programmed to acquire full scan mass spectra (m/z 300-2000) in profile mode (spray voltage = 4.5 kV). Mass spectra were deconvoluted using MagTran software version 1.03b2[25].

To identify the site of covalent modification, MFH290 treated CDK/Cyclin K complex was reduced with 10 mM tris(2-carboxyethyl)phosphine for 10 minutes at room temperature, alkylated with 20 mM methyl methanethiosulfonate for 10 minutes at room temperature, and digested with Glu-C protease (Promega, Madison, WI) overnight at 37 °C. Peptides were desalted using C18 (SOLA, ThermoFisher Scientific, Madison, WI), dried by vacuum centrifugation, reconstituted in 50% acetonitrile, 1% formic acid, 100 mM ammonium acetate, and analyzed by CE-MS using a ZipChip CE-MS instrument and autosampler (908 devices, Boston, MA) interfaced to a QExactive HF mass spectrometer (ThermoFisher Scientific). Peptides were resolved at 500V/cm using an HR chip with a background electrolyte consisting of 50% acetonitrile with 1% formic acid. The mass spectrometer was operated in data dependent mode, and subjected the 5 most abundant ions in each MS scan (m/z 300-2000, 60K resolution, 3E6 target, 100 ms max fill time) to MS/MS (15K resolution, 1E5 target, 100 ms max fill time). Dynamic exclusion was enabled with a repeat count of 1 and an exclusion duration of 5 seconds. Raw mass

spectrometry data files were converted to .mgf using multiplierz software[26] and searched against a forward-reverse human refseq database using Mascot version 2.6.2. Search parameters specified fixed methylthio modification of cysteine, variable methionine oxidation, and variable MFH290 modification of cysteine. MFH290 modified spectra were examined and figures prepared using mzStudio software[27]. MFH290 specific product ions were assigned as described[16].

RNA Extraction and Synthetic RNA Spike-In

Total RNA and sample preparation were performed as previously described[28]. Briefly, HAP1 cells were incubated in media containing MFH290 at the indicated concentrations or with DMSO for the specified duration of time. Cell numbers were determined by manually counting cells using C-Chip disposable hemocytometers (Digital Bio, DHC-N01) prior to lysis and RNA extraction. Total RNA from biological replicates (equivalent to 5 million cells per replicate) was subsequently isolated using RNeasy Plus Mini kit (Qiagen, cat#74134) following the manufacturer's instructions and re-suspended in 50 µL nuclease-free water (Ambion, AM9938).

cDNA Preparation and TaqMan Expression Analysis

RNA utilized for RT-PCR was extracted as outlined above. One microgram of purified RNA was reverse transcribed using Superscript III First-Strand (Invitrogen, cat# 18080-051) with oligo dT primers to prime first-strand synthesis according to the manufacturer's protocol. qPCR was carried out on the 7000 ABI Detection System using the following Taqman probes according to the manufacturer's protocol (Applied Biosystems). All experiments shown were performed in biological triplicate. Each individual biological

sample was qPCR-amplified in technical duplicate. Error bars are +/- SD. Expression was normalized to GAPDH, and fold change in expression was calculated relative to the indicated conditions. The following Taqman probes from Life Technologies were used for qPCR-based gene expression analysis: GAPDH - Hs02758991_g1; BRCA2 - Hs00609073_m1; RAD51 – Hs00947967_m1; and RAD51C - Hs00427442_m1.

In Vivo Pharmacokinetic Studies

Male Swiss albino mice were dosed with MFH290 solution formulation (intravenous, 5% NMP, 5% Solutol HS-15, 90% Normal saline, dose 1 mg/kg) or (Intraperitoneal 5% NMP, 5% Solutol, 90% Normal saline, dose 5 mg/kg) or (oral, 5% NMP, 5% Solutol HS-15, 90% Normal saline, dose 10 mg/kg). Blood samples were collected at Pre-dose, 0.08, 0.25, 0.5, 1, 2, 4, 8 and 24 hr (IV and IP) and Pre-dose, 0.25, 0.5, 1, 2, 4, 6, 8 and 24 hr (PO). The blood samples were collected from sets of three mice at each time point in labeled microcentrifuge tubes containing K2EDTA as an anticoagulant. Plasma samples were separated by centrifugation and stored below −70 °C until bioanalysis. All samples were processed for analysis by precipitation using acetonitrile and analyzed with a partially validated LC/MS/MS method (LLOQ - 1.22 ng/mL for IV and PO, LLOQ – 5.02 ng/mL for IP). Pharmacokinetic parameters were calculated using the noncompartmental analysis tool of WinNonlin Enterprise software (Version 6.3).

AUTHOR INFORMATION

Corresponding Author

*Email: NicholasP_Kwiatkowski@dfci.harvard.edu; *Email: Tinghu_Zhang@dfci.harvard.edu; *Email: Nathanael_Gray@dfci.harvard.edu.

Author Contributions

Conceptualization: N.G., T.Z.; Chemistry: Y.L., M.H., Z.H.; Biology: A.L., N.K. Y.G., C.O.; Computational: J. C.; Mass spectrum labeling: S.F., J.M.; Writings: T.Z., Y.L., N.K., N.G.; The manuscript was written through contributions of all authors. All authors have given approval to the final version of the manuscript. ‡These authors contributed equally. (match statement to author names with a symbol)

ACKNOWLEDGMENT

We thank Jim Sun at NMR facility of Dana-Farber cancer institute for his assistance on NMR data collection. Milka Kostic is greatly acknowledged for the editing and proof reading. This work was supported by Susan Smith Center for Women's Cancer – PPG Award and Dana-Farber Cancer Institute Accelerator grant.

ABBREVIATIONS

BRCA, Breast cancer gene; PDX, Patient-derived xenograft; HATU, 1-[Bis(dimethylamino)methylene]-1H-1,2,3-triazolo[4,5-b]pyridinium 3-oxid hexafluorophosphate, Hexafluorophosphate Azabenzotriazole Tetramethyl Uronium; Boc, *Tert*-butyloxycarbonyl; DIEA, N, N-Diisopropylethylamine; DMF, Dimethylformamide; DMAP, 4-Dimethylaminopyridine; EDCI, 1-Ethyl-3-(3-dimethylaminopropyl)carbodiimide; THF, Tetrahydrofuran; m-CPBA, meta-Chloroperbenzoic acid; NMP, N-Methyl-2-Pyrrolidone; HCl, Hydrochloric acid; MeOH, Methanol; Py, Pyridine; T_3P, Propylphosphonic Anhydride; DCM, Dichloromethane;

MeCN, Acetonitrile; KSCN, Potassium thiocyanate; *t*-BuOK, Potassium tert-butoxide; *t*-BuONO, tert-Butyl nitrite; WT, wild type; T-ALL, T-acute lymphoblastic leukemia; CML, Chronic myelogenous leukemia.

Conflict of Interest

N.S.G. is a founder, SAB and equity holder in Gatekeeper, Syros, Petra, C4, B2S and Soltego. The Gray lab receives/has received funding from Novartis, Takeda, Astellas, Taiho, Janssen, Kinogen, Voronoi, Her2llc, Deerfield and Sanofi.

ASSOCIATED CONTENT

Supporting Information

The Supporting Information is available free of charge on the XXXX.

Schematic of target engagement experiment (Figure S1A); Known CDK inhibitors screened by target engagement assay (Figure S1B); Structure activity relationship (SAR) screen of covalent compounds using target engagement assay (Figure S2); MFH290 targets CDK12 and CDK13 in cells (Figure S3); CRISPR technique mutates Cys-1039 to serine (C1039S) at CDK12 loci and Cys-1017 to serine (C1017S) at CDK13 loci (Figure S4A); Western blot of CDK12 and CDK13 WT and Cys-to-Ser mutants in HAP1 cells (Figure S4B); KinomeScan profiling data for MFH290 (Table S1); 1H NMR spectrum of compound MFH290 (Figure S5A); HPLC spectrum of compound MFH290 (Figure S5B); LC-MS spectrum of compound MFH290 (Figure S5C)

Overlay of SNS032/CDK2 (PDB code: 5D1J) and CDK12 (PDB code: 5ACB) (PDB)

Molecular formula strings (CSV)

REFERENCES

1. Malumbres, M.; Barbacid, M. Cell Cycle, CDKs and Cancer: a Changing Paradigm. *Nature Reviews Cancer* **2009,** *9*, 153-166.

2. Hydbring, P.; Malumbres, M.; Sicinski, P. Non-Canonical Functions of Cell Cycle Cyclins and Cyclin-Dependent Kinases. *Nature Reviews Molecular Cell Biology* **2016,** *17*, 280-292.

3. Asghar, U.; Witkiewicz, A. K.; Turner, N. C.; Knudsen, E. S. The History and Future of Targeting Cyclin-Dependent Kinases in Cancer Therapy. *Nature Reviews Drug Discovery* **2015,** *14*, 130-146.

4. Kwiatkowski, N.; Zhang, T.; Rahl, P. B.; Abraham, B. J.; Reddy, J.; Ficarro, S. B.; Dastur, A.; Amzallag, A.; Ramaswamy, S.; Tesar, B.; Jenkins, C. E.; Hannett, N. M.; McMillin, D.; Sanda, T.; Sim, T.; Kim, N. D.; Look, T.; Mitsiades, C. S.; Weng, A. P.; Brown, J. R.; Benes, C. H.; Marto, J. A.; Young, R. A.; Gray, N. S. Targeting Transcription Regulation in Cancer with a Covalent CDK7 Inhibitor. *Nature* **2014,** *511*, 616-620.

5. Zhang, T.; Kwiatkowski, N.; Olson, C. M.; Dixon-Clarke, S. E.; Abraham, B. J.; Greifenberg, A. K.; Ficarro, S. B.; Elkins, J. M.; Liang, Y.; Hannett, N. M.; Manz, T.; Hao, M.; Bartkowiak, B.; Greenleaf, A. L.; Marto, J. A.; Geyer, M.; Bullock, A. N.; Young, R. A.; Gray, N. S. Covalent Targeting of Remote Cysteine Residues to Develop CDK12 and CDK13 Inhibitors. *Nature Chemical Biology* **2016,** *12*, 876-884.

6. Cheng, S. W.; Kuzyk, M. A.; Moradian, A.; Ichu, T. A.; Chang, V. C.; Tien, J. F.; Vollett, S. E.; Griffith, M.; Marra, M. A.; Morin, G. B. Interaction of Cyclin-Dependent Kinase 12/CrkRS with Cyclin K1 Is Required for the Phosphorylation of the C-terminal Domain of RNA Polymerase II. *Molecular and Cellular Biology* **2012,** *32*, 4691-4704.

7. Joshi, P. M.; Sutor, S. L.; Huntoon, C. J.; Karnitz, L. M. Ovarian Cancer-Associated Mutations Disable Catalytic Activity of CDK12, a Kinase That Promotes Homologous Recombination Repair and Resistance to Cisplatin and Poly (ADP-ribose) polymerase Inhibitors. *Journal of Biological Chemistry* **2014,** *289*, 9247-9253.

8. Bartkowiak, B.; Yan, C.; Greenleaf, A. L. Engineering an Analog-Sensitive CDK12 Cell Line Using CRISPR/Cas. *Biochimica et Biophysica Acta Gene Regulatory Mechanisms* **2015,** *1849*, 1179-1187.

9. Bajrami, I.; Frankum, J. R.; Konde, A.; Miller, R. E.; Rehman, F. L.; Brough, R.; Campbell, J.; Sims, D.; Rafiq, R.; Hooper, S.; Chen, L.; Kozarewa, I.; Assiotis, I.; Fenwick, K.; Natrajan, R.; Lord, C. J.; Ashworth, A. Genome-Wide Profiling of Genetic Synthetic Lethality Identifies CDK12 as a Novel Determinant of PARP1/2 Inhibitor Sensitivity. *Cancer Research* **2014,** *74*, 287-297.

10. Johnson, S. F.; Cruz, C.; Greifenberg, A. K.; Dust, S.; Stover, D. G.; Chi, D.; Primack, B.; Cao, S.; Bernhardy, A. J.; Coulson, R.; Lazaro, J.-B.; Kochupurakkal, B.; Sun, H.; Unitt, C.; Moreau, L. A.; Sarosiek, K. A.; Scaltriti, M.; Juric, D.; Baselga, J.; Richardson, A. L.; Rodig, S. J.; D'Andrea, A. D.; Balmaña, J.; Johnson, N.; Geyer, M.; Serra, V.; Lim, E.; Shapiro, G. I. CDK12 Inhibition Reverses De Novo and Acquired PARP Inhibitor Resistance in BRCA Wild-Type and Mutated Models of Triple-Negative Breast Cancer. *Cell Reports* **2016,** *17*, 2367-2381.

11. Paruch, K.; Dwyer, M. P.; Alvarez, C.; Brown, C.; Chan, T.-Y.; Doll, R. J.; Keertikar, K.; Knutson, C.; McKittrick, B.; Rivera, J.; Rossman, R.; Tucker, G.; Fischmann, T.; Hruza, A.; Madison, V.; Nomeir, A. A.; Wang, Y.; Kirschmeier, P.; Lees, E.; Parry, D.; Sgambellone, N.; Seghezzi, W.; Schultz, L.; Shanahan, F.; Wiswell, D.; Xu, X.; Zhou, Q.;

James, R. A.; Paradkar, V. M.; Park, H.; Rokosz, L. R.; Stauffer, T. M.; Guzi, T. J. Discovery of Dinaciclib (SCH 727965): a Potent and Selective Inhibitor of Cyclin-Dependent Kinases. *ACS Medicinal Chemistry Letters* **2010,** *1*, 204-208.

12. Johannes, J. W.; Denz, C. R.; Su, N.; Wu, A.; Impastato, A. C.; Mlynarski, S.; Varnes, J. G.; Prince, D. B.; Cidado, J.; Gao, N.; Haddrick, M.; Jones, N. H.; Li, S.; Li, X.; Liu, Y.; Nguyen, T. B.; O'Connell, N.; Rivers, E.; Robbins, D. W.; Tomlinson, R.; Yao, T.; Zhu, X.; Ferguson, A. D.; Lamb, M. L.; Manchester, J. I.; Guichard, S. Structure-Based Design of Selective Noncovalent CDK12 Inhibitors. *ChemMedChem* **2018,** *13*, 231-235.

13. Ito, M.; Tanaka, T.; Toita, A.; Uchiyama, N.; Kokubo, H.; Morishita, N.; Klein, M. G.; Zou, H.; Murakami, M.; Kondo, M.; Sameshima, T.; Araki, S.; Endo, S.; Kawamoto, T.; Morin, G. B.; Aparicio, S. A.; Nakanishi, A.; Maezaki, H.; Imaeda, Y. Discovery of 3-Benzyl-1-(trans-4-((5-cyanopyridin-2-yl) amino) cyclohexyl)-1-arylurea Derivatives as Novel and Selective Cyclin-Dependent Kinase 12 (CDK12) Inhibitors. *Journal of Medicinal Chemistry* **2018,** *61*, 7710-7728.

14. Quereda, V.; Bayle, S.; Vena, F.; Frydman, S. M.; Monastyrskyi, A.; Roush, W. R.; Duckett, D. R. Therapeutic Targeting of CDK12/CDK13 in Triple-Negative Breast Cancer. *Cancer Cell* **2019,** *36*, 545-558.e7.

15. Misra, R. N.; Xiao, H.-y.; Kim, K. S.; Lu, S.; Han, W.-C.; Barbosa, S. A.; Hunt, J. T.; Rawlins, D. B.; Shan, W.; Ahmed, S. Z.; Qian, L.; Chen, B.-C.; Zhao, R.; Bednarz, M. S.; Kellar, K. A.; Mulheron, J. G.; Batorsky, R.; Roongta, U.; Kamath, A.; Marathe, P.; Ranadive, S. A.; Sack, J. S.; Tokarski, J. S.; Pavletich, N. P.; Lee, F. Y. F.; Webster, K. R.; Kimball, S. D. *N*-(Cycloalkylamino) acyl-2-aminothiazole Inhibitors of Cyclin-Dependent Kinase 2. *N*-[5-[[[5-(1, 1-dimethylethyl)-2-oxazolyl] methyl] thio]-2-thiazolyl]-4-

piperidinecarboxamide (BMS-387032), a Highly Efficacious and Selective Antitumor Agent. *Journal of Medicinal Chemistry* **2004,** *47*, 1719-1728.

16. Ficarro, S. B.; Browne, C. M.; Card, J. D.; Alexander, W. M.; Zhang, T.; Park, E.; McNally, R.; Dhe-Paganon, S.; Seo, H.-S.; Lamberto, I.; Eck, M. J.; Buhrlage, S. J.; Gray, N. S.; Marto, J. A. Leveraging Gas-Phase Fragmentation Pathways for Improved Identification and Selective Detection of Targets Modified by Covalent Probes. *Analytical Chemistry* **2016,** *88*, 12248-12254.

17. Fabian, M. A.; Biggs, W. H., 3rd; Treiber, D. K.; Atteridge, C. E.; Azimioara, M. D.; Benedetti, M. G.; Carter, T. A.; Ciceri, P.; Edeen, P. T.; Floyd, M.; Ford, J. M.; Galvin, M.; Gerlach, J. L.; Grotzfeld, R. M.; Herrgard, S.; Insko, D. E.; Insko, M. A.; Lai, A. G.; Lélias, J.-M.; Mehta, S. A.; Milanov, Z. V.; Velasco, A. M.; Wodicka, L. M.; Patel, H. K.; Zarrinkar, P. P.; Lockhart, D. J. A Small Molecule–Kinase Interaction Map for Clinical Kinase Inhibitors. *Nature Biotechnology* **2005,** *23*, 329-336.

18. Karaman, M. W.; Herrgard, S.; Treiber, D. K.; Gallant, P.; Atteridge, C. E.; Campbell, B. T.; Chan, K. W.; Ciceri, P.; Davis, M. I.; Edeen, P. T.; Faraoni, R.; Floyd, M.; Hunt, J. P.; Lockhart, D. J.; Milanov, Z. V.; Morrison, M. J.; Pallares, G.; Patel, H. K.; Pritchard, S.; Wodicka, L. M.; Zarrinkar, P. P. A Quantitative Analysis of Kinase Inhibitor Selectivity. *Nature Biotechnology* **2008,** *26*, 127-132.

19. Bartkowiak, B.; Liu, P.; Phatnani, H. P.; Fuda, N. J.; Cooper, J. J.; Price, D. H.; Adelman, K.; Lis, J. T.; Greenleaf, A. L. CDK12 Is a Transcription Elongation-Associated CTD Kinase, the Metazoan Ortholog of Yeast Ctk1. *Genes Development* **2010,** *24*, 2303-2316.

20. Blazek, D.; Kohoutek, J.; Bartholomeeusen, K.; Johansen, E.; Hulinkova, P.; Luo, Z.; Cimermancic, P.; Ule, J.; Peterlin, B. M. The Cyclin K/Cdk12 Complex Maintains Genomic Stability via Regulation of Expression of DNA Damage Response Genes. *Genes & Development* **2011,** *25*, 2158-2172.

21. Liu, Y.; Burness, M. L.; Martin-Trevino, R.; Guy, J.; Bai, S.; Harouaka, R.; Brooks, M. D.; Shang, L.; Fox, A.; Luther, T. K.; Davis, A.; Baker, T. L.; Colacino, J.; Clouthier, S. G.; Shao, Z.-M.; Wicha, M. S.; Liu, S. RAD51 Mediates Resistance of Cancer Stem Cells to PARP Inhibition in Triple-Negative Breast Cancer. *Clinical Cancer Research* **2017,** *23*, 514-522.

22. Bliss, C. The Calculation of Microbial Assays. *Bacteriological Reviews* **1956,** *20*, 243-258.

23. Greco, W. R.; Bravo, G.; Parsons, J. C. The Search for Synergy: a Critical Review from a Response Surface Perspective. *Pharmacological Reviews* **1995,** *47*, 331-385.

24. Choong, I. C.; Serafimova, I.; Fan, J.; Stockett, D.; Chan, E.; Cheeti, S.; Lu, Y.; Fahr, B.; Pham, P.; Arkin, M. R.; Walker, D. H.; Hoch, U. A Diaminocyclohexyl Analog of SNS-032 with Improved Permeability and Bioavailability Properties. *Bioorganic Medicinal Chemistry Letters* **2008,** *18*, 5763-5765.

25. Zhang, Z.; Marshall, A. G. A Universal Algorithm for Fast and Automated Charge State Deconvolution of Electrospray Mass-to-Charge Ratio Spectra. *Journal of the American Society for Mass Spectrometry* **1998,** *9*, 225-233.

26. Alexander, W. M.; Ficarro, S. B.; Adelmant, G.; Marto, J. Multiplierz V2.0: A Python-Based Ecosystem for Shared Access and Analysis of Native Mass Spectrometry Data. *Proteomics* **2017,** *17*, 15-16.

27. Ficarro, S.; Alexander, W.; Marto, J. MzStudio: a Dynamic Digital Canvas for User-Driven Interrogation of Mass Spectrometry Data. *Proteomes* **2017,** *5*, 20.

28. Lovén, J.; Orlando, D. A.; Sigova, A. A.; Lin, C. Y.; Rahl, P. B.; Burge, C. B.; Levens, D. L.; Lee, T. I.; Young, R. A. Revisiting Global Gene Expression Analysis. *Cell* **2012,** *151*, 476-482.

Table of Contents graphic

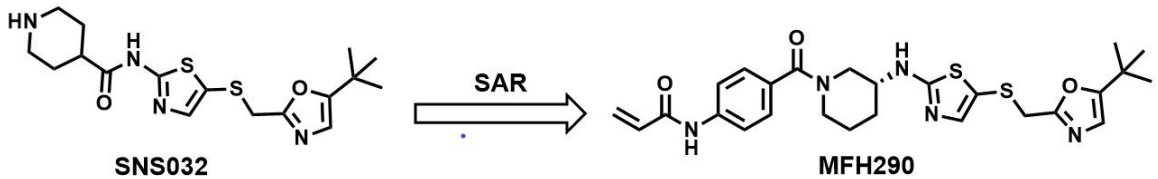

SNS032

CDK2/7/9 reversible inhibitor

CDK2/cyclin A	IC_{50} = 21 nM
CDK7/cyclin H/MNAT1	IC_{50} = 184 nM
CDK9/cyclin T1	IC_{50} = 6 nM

MFH290

selective CDK12/13 covalent inhibitor

only hit CDK13 in a panel of 468 human kinases

CDK2/cyclin A	IC_{50} = 120 nM
CDK7/cyclin H/MNAT1	IC_{50} = 6020 nM
CDK9/cyclin T1	IC_{50} = 114 nM